

# Models for the Photosynthetic Reaction Center: Preparation, Spectroscopy, and Crystal and Molecular Structures of Cofacial Bisporphyrins Linked by *cis*-1,2- and *trans*-1,2-Ethene Bridges and of 1,1-Carbinol-Bridged Bisporphyrins

Mathias O. Senge, M. Graça H. Vicente, Kevin R. Gerzevske, Timothy P. Forsyth, and Kevin M. Smith\*

Department of Chemistry, University of California, Davis, California 95616

Received March 2, 1994<sup>®</sup>

The low-valent titanium induced reductive coupling of metal(II) 5-formyl-octaethylporphyrin (OEP) (**2**, **3**) leads to the formation of ethene-bridged bisporphyrins. Structural studies on the main products of the coupling of Cu(II) (**2**) and Ni(II) 5-formyl-OEP (**3**) revealed, surprisingly, the formation of the *cis*-isomers 1,2-bis[5-(2,3,7,8,12,13,17,18-octaethylporphyrinato)metal(II)]-*cis*-ethene (**4**, **5**). This is in contrast to other reported reductive couplings of aldehydes and ketone which usually lead to the *trans*-product. The *cis*-isomer can undergo an acid-catalyzed isomerization to the *trans*-isomer (**6**, **7**) which is also formed as a side product in the coupling reaction. An explanation for the formation of the *cis*-ethene-bridged bisporphyrins may involve the strong aggregation tendencies of metalloporphyrins. These aggregation forces are evidenced in the crystal structures of the *cis*-dimers which exhibit considerable overlap of the  $\pi$ -systems and have a cofacial macrocycle arrangement with almost coplanar macrocycles. Besides the strong intramolecular aggregation effects, intermolecular  $\pi$ -stacking was observed in the structures of the Cu(II) (**4**) and Ni(II) (**5**) *cis*-dimers, the nickel(II) *trans*-isomer (**7**) and the related structure of bis[2-(3,7,8,12,13,17,18-heptaethylporphyrinato)nickel(II)]hydroxymethane (**13**) which is obtained by low valent titanium coupling of Ni(II) 2-formyl-OEP (**12**). The synthesis of the cofacial *cis*-dimers is achieved in a single step from the corresponding formylporphyrins in high yields, thus presenting an improvement over other published procedures for synthesis of face-to-face bisporphyrins. Crystal data: **4**, Mo K $\alpha$  ( $\lambda = 0.71069 \text{ \AA}$ ) at 130 K,  $a = 19.208(7) \text{ \AA}$ ,  $b = 14.672(5) \text{ \AA}$ ,  $c = 24.170(7) \text{ \AA}$ ,  $\beta = 111.15(3)^\circ$ ,  $V = 6352(4) \text{ \AA}^3$ ,  $Z = 4$ , space group  $P2_1/n$ ,  $R = 0.056$ ; **5**, Mo K $\alpha$  ( $\lambda = 0.71069 \text{ \AA}$ ) at 130 K,  $a = 21.671(7) \text{ \AA}$ ,  $b = 14.079(5) \text{ \AA}$ ,  $c = 22.110(7) \text{ \AA}$ ,  $\beta = 108.86(2)^\circ$ ,  $V = 6384(3) \text{ \AA}^3$ ,  $Z = 4$ , space group  $P2_1/c$ ,  $R = 0.064$ ; **7**, Cu K $\alpha$  ( $\lambda = 1.54178 \text{ \AA}$ ) at 126 K,  $a = 11.163(3) \text{ \AA}$ ,  $b = 12.775(4) \text{ \AA}$ ,  $c = 14.554(3) \text{ \AA}$ ,  $\alpha = 69.59(2)^\circ$ ,  $\beta = 81.15(2)^\circ$ ,  $\gamma = 73.21(2)^\circ$ ,  $V = 1859(1) \text{ \AA}^3$ ,  $Z = 1$ , space group  $P\bar{1}$ ,  $R = 0.072$ ; **13**, Mo K $\alpha$  ( $\lambda = 0.71069 \text{ \AA}$ ) at 130 K,  $a = 40.31(2) \text{ \AA}$ ,  $b = 14.997(7) \text{ \AA}$ ,  $c = 21.954(11) \text{ \AA}$ ,  $\beta = 108.6(4)^\circ$ ,  $V = 12579(10) \text{ \AA}^3$ ,  $Z = 8$ , space group  $C2/c$ ,  $R = 0.122$ .

## Introduction

Covalently linked porphyrin dimers are of central importance for understanding the primary processes of photosynthesis,<sup>1</sup> are studied with regard to their ability to catalytically reduce water,<sup>2</sup> and have potential for use as photosensitizers in photodynamic therapy.<sup>3</sup> We are mainly interested in the preparation and characterization of bisporphyrins as models for the photosynthetic reaction center. As shown by the X-ray crystal structures of the bacterial photosynthetic reaction center, the most prominent characteristic of the special pair is the cofacial arrangement of the two bacteriochlorophylls involved and their electronic coupling.<sup>4</sup>

Model systems are often used to facilitate studies; in the present case the geometry of the subunits in a dimer must be known, and preferably the relative arrangement of the subunits

should be varied to enable studies of the effects of interplanar separation and spatial arrangement. A comparative analysis of systems with linear extended, skewed, and cofacial subunit arrangement would be of interest. Over the years many examples of systems with linear extended porphyrin structures have been prepared and studied.<sup>1,5</sup> Structurally characterized examples include ethane-bridge Ni<sup>II</sup>OEP,<sup>5b</sup> 1,2-bis(5-octaethylchlorin)ethane,<sup>5c</sup> and 10,10-dithiobis(coproporphyrin II tetramethyl ester).<sup>5d</sup> Similarly, several examples of bisporphyrins with skewed orientations relative to each other (gable-porphyrins) have been prepared.<sup>2b,6</sup> A recent example of a structurally characterized gable-bisporphyrin is [5,5'-(furan-

<sup>®</sup> Abstract published in *Advance ACS Abstracts*, November 1, 1994.

- (1) Wasielewski, M. R. *Photochem. Photobiol.* **1988**, *47*, 923; *Chem. Rev.* **1992**, *92*, 435. Gust, D.; Moore, T. A. *Top. Curr. Chem.* **1991**, *159*, 103.
- (2) Collman, J. P.; Anson, F. C.; Barnes, C. E.; Bencosme, C. S.; Geiger, T.; Evtitt, E. R.; Kreh, R. P.; Meier, K.; Pettman, R. B. *J. Am. Chem. Soc.* **1983**, *105*, 2694. (b) Naruta, Y.; Sasayama, M.; Maruyama, K. *Chem. Lett.* **1992**, 1267.
- (3) Kessel, D.; Dougherty, T. J.; Chang, C. K. *Photochem. Photobiol.* **1991**, *53*, 475.
- (4) (a) Deisenhofer, J.; Epp, O.; Miki, K.; Huber, R.; Michel, H. *J. Mol. Biol.* **1984**, *180*, 385. Deisenhofer, J.; Michel, H. *Angew. Chem., Int. Ed. Engl.* **1989**, *28*, 829. (b) Allen, J. P.; Feher, G.; Yeates, T. O.; Komiyama, H.; Rees, R. C. *Proc. Natl. Acad. Sci. U.S.A.* **1988**, *85*, 8487.

- (5) (a) Johnson, S. G.; Svec, W. A.; Wasielewski, M. R. *Isr. J. Chem.* **1988**, *28*, 193. Sessler, J. L.; Johnson, M. R.; Creager, S. F.; Fetting, J. C.; Ibers, J. A. *J. Am. Chem. Soc.* **1990**, *112*, 9310. (b) Hitchcock, P. B. *J. Chem. Soc., Dalton Trans.* **1983**, 2127. (c) Senge, M. O.; Hope, H.; Smith, K. M. *J. Chem. Soc., Perkin Trans. 2* **1993**, 11. (d) Clezy, P. S.; Craig, D. C.; James, V. J.; McConnell, J. F.; Rae, A. D. *Cryst. Struct. Commun.* **1979**, *8*, 605. (e) Osuka, A.; Tanabe, N.; Zhang, R. P.; Maruyama, K. *Chem. Lett.* **1993**, 1505. Anderson, H. L. *Inorg. Chem.* **1994**, *33*, 972. Anderson, H. L.; Martin, S. J.; Bradley, D. D. C. *Angew. Chem., Int. Ed. Engl.* **1994**, *33*, 655.
- (6) (a) Tabushi, I.; Sasaki, T. *Tetrahedron Lett.* **1982**, *23*, 1913. (b) Osuka, A.; Maruyama, K. *Chem. Lett.* **1987**, 825. Rodriguez, J.; Kirmaier, C.; Johnson, M. R.; Friesner, R. A.; Holten, D.; Sessler, J. L. *J. Am. Chem. Soc.* **1991**, *113*, 1652. (c) Arnold, D. P.; Lynch, D. E.; Smith, G.; Kennard, C. H. L. *Aust. J. Chem.* **1993**, *46*, 1313. (d) Meier, H.; Kobuke, Y.; Kugimiyama, S.-i. *J. Chem. Soc., Chem. Commun.* **1989**, 923. Arnold, D. P.; Nitschinsk, L. J. *Tetrahedron Lett.* **1993**, *34*, 693. (e) Sessler, J. L.; Johnson, M. R.; Creager, S. E.; Fetting, J. C.; Ibers, J. A. *J. Am. Chem. Soc.* **1990**, *112*, 9310.

2,5-diyl)bis(OEP)],<sup>6c</sup> Most important, however, are the bis-porphyrins with a face-to-face arrangement of their macrocycles. A variety of such cofacial dimers have been prepared, beginning with the pioneering work of Collman et al. on *meso*-tetraaryl-substituted systems,<sup>7a</sup> followed by their work on face-to-face porphyrins with 5,15-<sup>7b</sup> and 2,12-linkages.<sup>7c,d</sup> Variations in the interplanar distances in systems with cofacial orientation has been achieved by coupling the porphyrins with two or more straps or by using rigid bridging units such as biphenylenediyl, anthracenediyl<sup>8d,e</sup> or 1,2-phenylene.<sup>8f-h</sup> Despite considerable efforts spent on these systems, definitive results have been obtained from their crystal structures for only a few examples.<sup>7bd,8bce,g,9</sup> Nevertheless, a detailed understanding of the exact geometrical arrangement of the subunits and their conformation is crucial for correct interpretation of the physicochemical properties and to correctly correlate such data with the situation *in vivo*. Besides the limited amount of structural information on bisporphyrins, another limitation in the study of biomimetic bisporphyrin models of the bacterial photosynthetic reaction center relates to their laborious preparation, usually involving numerous steps plagued with low yields.

Recently, it was shown that the low-valent titanium-induced reductive coupling (McMurry reaction)<sup>10</sup> of 5-formylporphyrins, which are easily derived from simple porphyrins, provides a convenient access to CH=CH-bridged bis-porphyrins.<sup>11</sup> Originally it was assumed that in all cases the products have the *trans*-configuration about the connecting double bond, as is usually observed in reductive couplings of aldehydes and ketones.<sup>10b</sup> This would lead to bisporphyrins with extended, linear structures. Preliminary results showed, however, that this method provides ready and convenient access to cofacial, *cis*-ethene-bridged dimers with a face-to-face arrangement.<sup>12</sup> Here we give full details of our studies on the 1,2-bis(5-2,3,7,8,12-, 13,17,18-octaethylporphyrinato)metal(II)]ethene dimers, present novel structural data for the nickel(II) *cis*- and *trans*-ethene dimers, and give a comparative analysis of the inter- and intramolecular  $\pi$ -interactions in the different dimers.

## Experimental Section

**General Methods.** Melting points were measured on a Thomas/Bristoline microscopic hot stage apparatus and are uncorrected. Silica gel 60 (70–230 and 230–400 mesh, Merck) was used for column chromatography. Analytical thin layer chromatography was performed using Merck 60 F254 silica gel (precoated sheets, 0.2 mm thick). <sup>1</sup>H-NMR spectra were obtained in deuteriochloroform solution at 300 MHz using a General Electric QE300 spectrometer; chemical shifts are expressed in ppm relative to chloroform (7.258 ppm). Elemental analyses were performed at the Midwest Microlab, Indianapolis, IN. Electronic absorption spectra were measured in dichloromethane solution using a Hewlett-Packard 8450A spectrophotometer. Mass spectra were obtained at the Mass Spectrometry Facility, University of California, San Francisco.

2,3,7,8,12,13,17,18-Octaethylporphyrin (**1**), (2,3,7,8,12,13,17,18-octaethylporphyrinato)copper(II), (2,3,7,8,12,13,17,18-octaethylporphyrinato)nickel(II), (2,3,7,8,12,13,17,18-octaethyl-5-formylporphyrinato)nickel(II) (**2**), and (2,3,7,8,12,13,17,18-octaethyl-5-formylporphyrinato)nickel(II) (**3**) were prepared according to published procedures.<sup>13</sup> Data for 1,2-bis[5-(2,3,7,8,12,13,17,18-octaethylporphyrinato)copper(II)]-*cis*-ethene, **4**, have already been given.<sup>11b</sup>

**Synthesis of *cis*- and *trans*-Nickel Dimers.** A 360 mg amount of TiCl<sub>3</sub>(DME)<sub>1.5</sub> and 240 mg of Zn/Cu couple were added to a dry helium filled flask in a drybox. A 10 mL volume of DME was added to the reaction flask, and the resulting mixture was refluxed for 2 h under an atmosphere of nitrogen to prepare the Ti<sup>0</sup> reagent. A solution of (5-formyl-2,3,7,8,12,13,17,18-octaethylporphyrinato)nickel(II) (100 mg, 0.147 mmol) in 10 mL of DMF was then added via a dropping funnel, and the reaction was complete after 30 min. The mixture was cooled to RT (room temperature), filtered through a fritted glass funnel, and the solid was washed with methylene chloride to dissolve any *cis*-isomer which had remained on the metal and salts. The solvent was removed *in vacuo*, and the solid was washed with 10% CH<sub>2</sub>Cl<sub>2</sub> in petroleum ether (40–60° fraction) to dissolve *cis*-isomer and keep the *trans*-isomer in the solid form. After concentrating the organic layer with the *cis*-isomer, chromatography on a flash silica gel column eluting with CH<sub>2</sub>Cl<sub>2</sub> in petroleum ether afforded Ni<sup>II</sup>OEP as the least polar band, followed by the *cis*-isomer which was concentrated and washed with methanol to yield 29.6 mg (33%).

The previously insoluble material was recrystallized from CH<sub>2</sub>Cl<sub>2</sub>/petroleum ether to afford 29 mg of crude *trans*-isomer. The metal and salts were again washed with THF to further dissolve any previously insoluble *trans*-isomer. The THF layer was combined with all previous remaining eluants. After concentration, a flash silica gel column eluting with 20% CH<sub>2</sub>Cl<sub>2</sub> in petroleum ether (a small amount of THF was added to the solid to aid in solubility prior to chromatography) yielded a small amount of Ni<sup>II</sup>OEP (total combined 6.5 mg). A solvent gradient finishing with neat CH<sub>2</sub>Cl<sub>2</sub> was necessary to elute the *trans*-isomer, which yielded 5.7 mg after recrystallization from CH<sub>2</sub>Cl<sub>2</sub>/CH<sub>3</sub>OH. Both fractions of the *trans*-isomer were combined to yield 34.7 mg (39%).

The overall yield of dimers was 73% with the *trans* to *cis* ratio being 1:2.

**1,2-Bis[5-(2,3,7,8,12,13,17,18-octaethylporphyrinato)nickel(II)]-*cis*-ethene, **5**:** Mp > 300 °C; UV/vis (CH<sub>2</sub>Cl<sub>2</sub>)  $\lambda_{\max}$  [nm] ( $\epsilon$ ) = 393 (168 000), 435 (12 200), 568 (14 700). <sup>1</sup>H-NMR (300 MHz, CDCl<sub>3</sub>, 25 °C):  $\delta$  = 9.30, 9.05 (s, 2 H each, *meso* and CH=CH), 8.06 (s, 4 H, *meso*), 4.03, 3.84, 3.75, 3.57, 3.47, 2.89 (m, 4 H each, CH<sub>2</sub>), 2.60 (s, 8 H, CH<sub>2</sub>), 1.83 (t, 12 H, CH<sub>3</sub>), 1.43–1.53 (m, 24 H, CH<sub>3</sub>), 0.67 (t, 12 H, CH<sub>3</sub>).

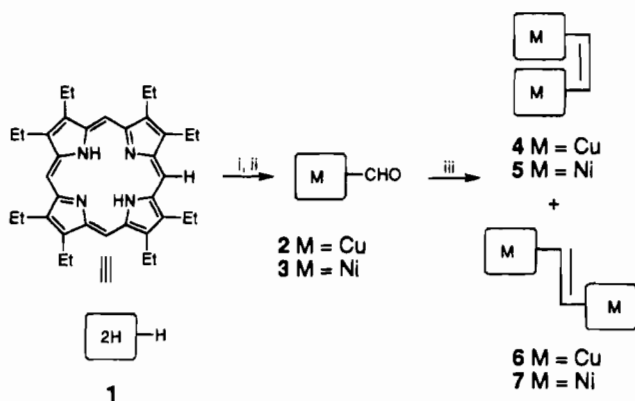
**1,2-Bis[5-(2,3,7,8,12,13,17,18-octaethylporphyrinato)nickel(II)]-*trans*-ethene, **7**:** Mp > 300 °C; UV/vis (CH<sub>2</sub>Cl<sub>2</sub>)  $\lambda_{\max}$  [nm] ( $\epsilon$ ) = 414 (160 000), 488 (30 400), 530 (20 700), 566 (22 800). <sup>1</sup>H-NMR (300 MHz, CDCl<sub>3</sub>, 25 °C):  $\delta$  = 9.50 (s, 2 H, *meso*), 9.48 (s, 4 H, *meso*), 7.66 (s, 2 H, CH=CH), 3.88 (m, 16 H, CH<sub>2</sub>), 3.76 (q, 8 H, CH<sub>2</sub>), 3.37 (m, br, 8 H, CH<sub>2</sub>), 1.83, 1.82, 1.75, 1.02 (t, 12 H each, CH<sub>3</sub>).

**X-ray Crystallographic Studies.** Crystals of **4** and **13** were grown by liquid diffusion of methanol into a concentrated solution of the porphyrin in CH<sub>2</sub>Cl<sub>2</sub>. Crystals of **5** and **7** were initially grown from CHCl<sub>3</sub>/hexanes. Crystals of **5** were frequently twinned, and a suitable crystal was found only after trying several different crystal batches.

- (7) (a) Collman, J. P.; Elliott, C. M.; Halbert, T. R.; Tovrog, B. S. *Proc. Natl. Acad. Sci. U.S.A.* **1977**, *74*, 18. (b) Collman, J. P.; Chong, A. O.; Jameson, G. B.; Oakley, R. T.; Rose, E.; Schmittou, E. R.; Ibers, J. A. *J. Am. Chem. Soc.* **1981**, *103*, 516. (c) Collman, J. P.; Anson, F. C.; Barnes, C. E.; Bencosme, C. S.; Geiger, T.; Evitt, E. R.; Kreh, R. P.; Meier, K.; Pettman, R. G. *J. Am. Chem. Soc.* **1983**, *105*, 2694. (d) Kim, K.; Collman, J. P.; Ibers, J. A. *J. Am. Chem. Soc.* **1988**, *110*, 4242.
- (8) (a) Chang, C. K.; Abdalmuhdi, I. *Angew. Chem., Int. Ed. Engl.* **1984**, *23*, 164. (b) Fillers, J. P.; Ravichandran, K. G.; Abdalmuhdi, I.; Tulinsky, A.; Chang, C. K. *J. Am. Chem. Soc.* **1986**, *108*, 417. (c) Collman, J. P.; Hutchison, J. E.; Lopez, M. A.; Tabard, A.; Guillard, R.; Seok, W. K.; Ibers, J. A.; L'Her, M. *J. Am. Chem. Soc.* **1992**, *114*, 9869. Guillard, R.; Lopez, M. A.; Tabard, A.; Richard, P.; Lecomte, C.; Brandes, S.; Hutchison, J. E.; Collman, J. P. *J. Am. Chem. Soc.* **1992**, *114*, 9877. (d) Chang, C. K.; Abdalmuhdi, I. *J. Org. Chem.* **1983**, *48*, 5388. (e) Nagata, T.; Osuka, A.; Maruyama, K. *J. Am. Chem. Soc.* **1990**, *112*, 3054. Osuka, A.; Nagata, T.; Maruyama, K. *Chem. Lett.* **1991**, 481. (f) Osuka, A.; Nakajima, S.; Maruyama, K. *J. Org. Chem.* **1992**, *57*, 7355. (g) Osuka, A.; Nakajima, S.; Nagata, T.; Maruyama, K.; Torumi, K. *Angew. Chem., Int. Ed. Engl.* **1991**, *30*, 582. (h) Meier, H.; Kobuke, Y.; Kugiyama, S.-i. *J. Chem. Soc., Chem. Commun.* **1989**, 108. Nagata, T.; Osuka, A.; Maruyama, K. *J. Am. Chem. Soc.* **1990**, *112*, 3054. Maruyama, K.; Osuka, A.; Mataga, N. *Pure Appl. Chem.* **1994**, *66*, 867.
- (9) (a) Hatada, M. H.; Tulinsky, A.; Chang, C. K. *J. Am. Chem. Soc.* **1980**, *102*, 7115. (b) Landrum, J. T.; Grimmett, D.; Haller, K. J.; Scheidt, W. R.; Reed, C. A. *J. Am. Chem. Soc.* **1981**, *103*, 2640. (c) Karaman, R.; Bruce, T. C. *J. Org. Chem.* **1991**, *56*, 3470.
- (10) (a) McMurry, J. E.; Lectka, T.; Rico, J. G. *J. Org. Chem.* **1989**, *54*, 3748. (b) McMurry, J. E. *Chem. Rev.* **1989**, *89*, 1513.
- (11) (a) Vicente, M. G. H.; Smith, K. M. *Synlett.* **1990**, 579. (b) *J. Org. Chem.* **1991**, *56*, 4407.
- (12) Senge, M. O.; Gerzevske, K. R.; Vicente, M. G. H.; Forsyth, T. P.; Smith, K. M. *Angew. Chem., Int. Ed. Engl.* **1993**, *32*, 750.

- (13) Smith, K. M., Ed. *Porphyrins and Metalloporphyrins*; Elsevier: Amsterdam, 1975.

## Scheme 1



<sup>a</sup> Reagents: i,  $M(OAc)_2$ ; ii,  $POCl_3/DMF$ ; iii,  $TiCl_3 \cdot DME_{1.5}$ ,  $Zn/Cu$  (McMurry coupling).

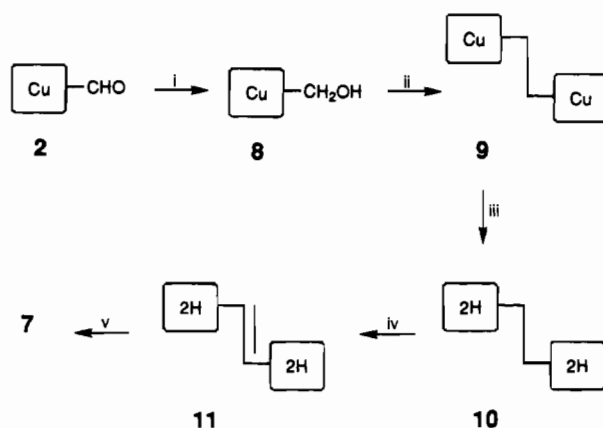
Although of apparent good quality crystals of **7** grown from chloroform/hexanes did not refine very well.<sup>12</sup> Finally crystals of good quality were obtained from toluene/hexanes.

The crystals were immersed in Paratone N oil; suitable single crystals were selected under a microscope, attached to a glass fiber and immediately placed in the low-temperature stream of the diffractometer.<sup>14</sup> Data sets for compounds **4** and **5** were collected at 130 K with the use of a Siemens R3m/V diffractometer (Mo  $K\alpha$  radiation,  $\lambda = 0.71069 \text{ \AA}$ ) equipped with a graphite monochromator and a locally modified Enraf-Nonius Universal low-temperature device. Data for **13** were collected on a Syntex P2<sub>1</sub> diffractometer (Mo  $K\alpha$  radiation,  $\lambda = 0.71069 \text{ \AA}$ ) equipped with a graphite monochromator and a locally modified Siemens low-temperature device. Data for **7** were collected with a Siemens P4 diffractometer equipped with a Siemens low-temperature device and a Siemens rotating anode (operating at 50 mA and 300 kV). Computer programs used for structure solution and refinements were those of SHELXTL-PLUS<sup>15</sup> installed on a Micro VAX station 3200. Scattering factors used were as supplied with SHELXTL. The structures of **7** and **13** were solved by a Patterson synthesis followed by structure expansion. The structures of **4** and **5** were solved by direct methods. The structures were refined by full matrix least-squares refinement and are corrected for Lorentz, polarization, and absorption effects.<sup>16</sup> Hydrogen atoms were included in the refinement at calculated positions using a riding model with  $C-H = 0.96 \text{ \AA}$ . All non-hydrogen atoms were refined with anisotropic thermal parameters. The structure of **13** is only of marginal quality. This is mainly due to bad crystal quality and disorder. One side chain ethyl atom [C(3B)] was disordered and was refined over two split positions with equal occupancy. The carbinol O atom was also found at two positions and was also refined over two positions with equal occupancy. Due to the limited data set only the Ni, N, and side chain atoms were refined with anisotropic thermal parameters.

## Results and Discussion

**Synthesis and Spectroscopy.** The first application of the McMurry reaction to the preparation of bisporphyrin was described 1991.<sup>11a</sup> In that study a number of different porphyrin dimers linked by alkene bridges were prepared. Initially the *trans*-configuration about the connecting double bond was assumed for the products of the coupling of porphyrins bearing

## Scheme 2



<sup>a</sup> Reagents: i,  $NaBH_4$ ; ii,  $CF_3CO_2H$ ; iii,  $H_2SO_4$ ; iv,  $CH_3CO_2H$ ,  $60^\circ C$ ; v,  $Ni(acac)_2$ .

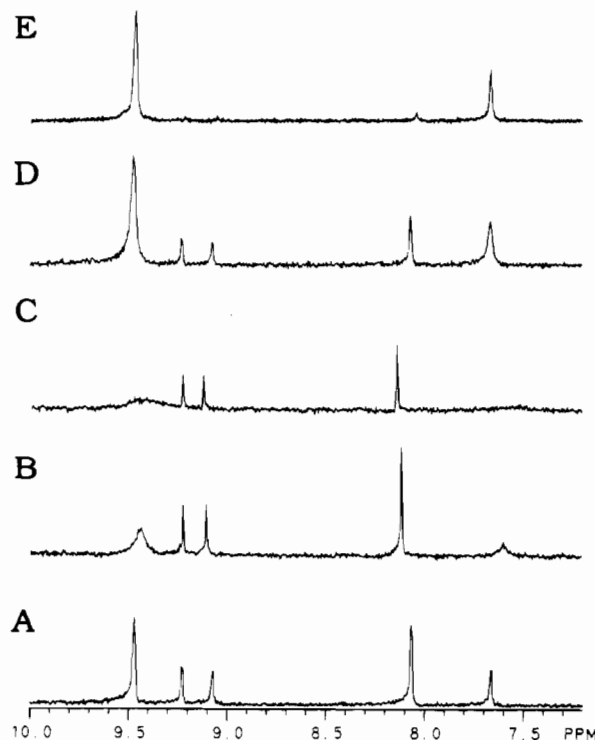
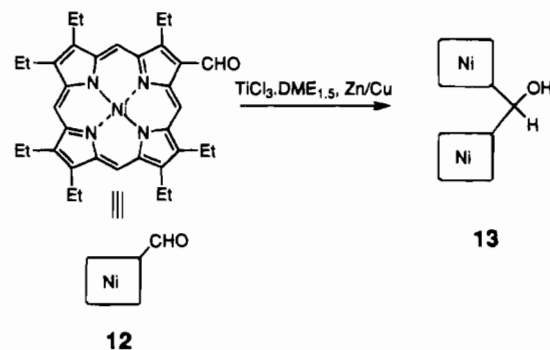


**Figure 1.** VT-NMR study in  $[D_2]$ -1,1,2,2-tetrachloroethane of McMurry mixture: (A) ambient to  $100^\circ C$ ; (B)  $110^\circ C$ ; (C)  $140^\circ C$ ; (D) back to  $40^\circ C$ ; (E) overnight at  $120^\circ C$ .

## Scheme 3



- (14) Hope, H. *ACS Symp. Ser.* **1987**, No. 357, 257.  
 (15) Sheldrick, G. M. *SHELXTL-PLUS, Program Package for Crystal Structure Solution and Refinement*; Universität Göttingen: Göttingen, Germany, 1989.  
 (16) Hope, H.; Moezzi, B. *Program XABS*; University of California: Davis, CA, 1987.  
 (17) Shul'ga, A. M.; Ponomarev, G. V. *Chem. Heterocycl. Compl. (Engl. Transl.)* **1986**, 22, 228; **1988**, 24, 276.  
 (18) Borovkov, V. V.; Ponomarev, G. V.; Ishida, A.; Kaneda, T.; Sakata, Y. *Chem. Lett.* **1993**, 1409.  
 (19) (a) Ponomarev, G. V.; Borovkov, V. V.; Sugiura, K.-i.; Sakata, Y.; Shul'ga, A. M. *Tetrahedron Lett.* **1993**, 34, 2153. (b) Kitagawa, R.; Kai, Y.; Ponomarev, G. V.; Sugiura, K.; Borovkov, V. V.; Kaneda, T.; Sakata, Y. *Chem. Lett.* **1993**, 1071.

*meso*-formyl functions though the proton NMR spectra (Figure 2B) of diamagnetic examples indicated a probable mixture of *cis* and *trans* isomers. A subsequent crystallographic study of the reaction product of the coupling of  $Cu(II)$  5-formyl-OEP (**2**) surprisingly showed that the isolated product had a *cis*-

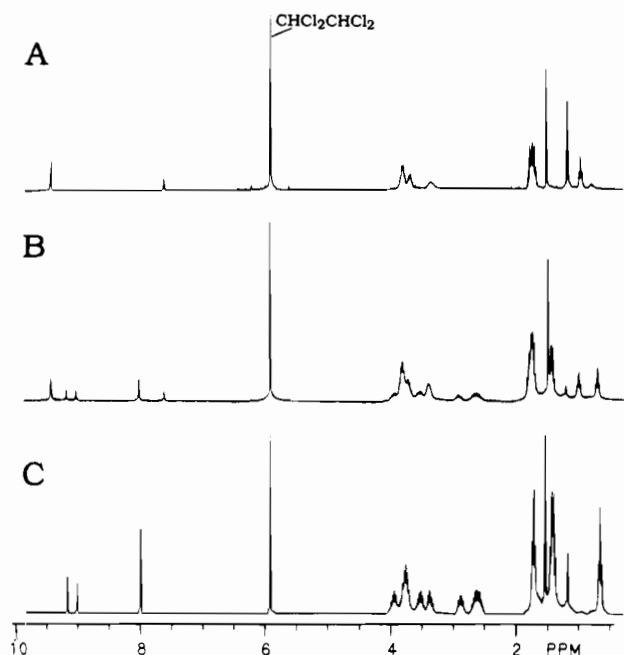


**Figure 2.** NMR-spectra of pure Ni-*cis*, pure Ni-*trans*, and McMurry Ni mixture: (A) pure *cis* (5); (B) McMurry Ni mixture; (C) pure *trans* (7).

configuration, i.e. structure 4.<sup>12</sup> Of note in the coupling of Ni(II) 5-formyl-OEP (3) were the UV/vis spectrum of the reaction product which showed the Soret band at 393 nm with a noticeable shoulder at longer wavelengths, and the NMR-spectrum exhibited a pattern more complex than should be expected for the symmetrical *trans*-isomer, 7.

Our first objective was the preparation of pure nickel(II) dimer, 5. Since initial attempts to demetallate, e.g. 4 with standard methodology (H<sub>2</sub>SO<sub>4</sub>/TFA) led to decomposition,<sup>11b</sup> we attempted to couple 5-formyl-OEP metalated with a more acid labile metal. After metalation of free base 5-formyl-OEP with either iron(III) chloride, zinc(II), or tin(II), these metal complexes were subjected to the low-valent titanium conditions. For the iron(II) complex, as many as three products were obtained, which after demetallation yielded only OEP as the major product. Attempts to dimerize Zn(II) 5-formyl-OEP led to substantial decomposition. Dimerization of Sn(II) 5-formyl-OEP also met with little success as well. Contrary to earlier reports<sup>11a</sup> immediate demetallation was observed in H<sub>2</sub>SO<sub>4</sub>/TFA. Spectrophotometry showed, however, a bathochromic shift (Soret band  $\lambda_{\max}$  = 418) compared with the *cis*-dimer ( $\lambda_{\max}$  = 390 nm). These data matched well with those obtained by Shul'ga and Ponomarev<sup>17</sup> on free-base 1,2-bis(5-2,3,7,8,12,13,17,18-octaethylporphyrin)-*trans*-ethene, prepared by a different route. Thus demetallation under the conditions used proceeded concurrently with *cis*  $\rightarrow$  *trans* isomerization.

Nickel(II) 5-formyl-OEP was subjected to the low valent titanium reductive coupling conditions to apparently give a single compound as demonstrated by TLC (accompanied by a small amount of Ni<sup>II</sup>OEP). Chromatography on silica gel, however, indicated inhomogeneity; a red nonpolar leading band was followed by a band which streaked, originating at the baseline of the column. Spectrophotometry of the compounds in the leading band showed an increased absorbance at  $\lambda_{\max}$  = 393 nm (Figure 3B) with no apparent bathochromically shifted shoulder, as described by Vicente and Smith.<sup>11b</sup> The compound obtained from the "streaking" band showed an absorbance at  $\lambda_{\max}$  = 414 nm (Figure 3A). The proton NMR spectrum of the nonpolar band clearly showed two products with one as the major product. In the *meso*-proton region, the peaks at 9.30,

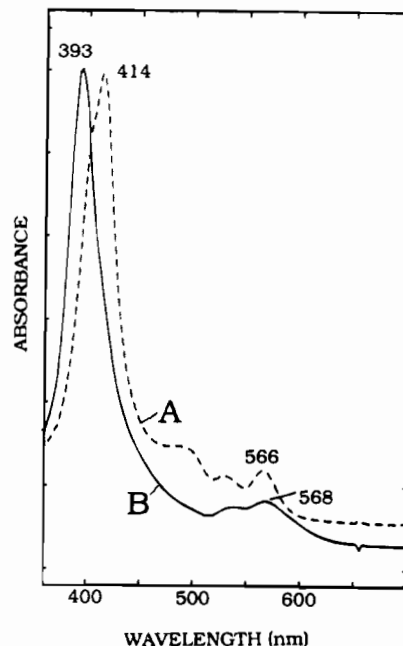


**Figure 3.** UV/vis spectrum of nickel *trans*-dimer (7) (A) dotted line and *cis*-dimer (5) (B, solid line).

9.05 and 8.06 ppm were more intense than the peaks at 9.50, 9.48, and 7.66 ppm (Figure 2B). The intensities were reversed for the products in the less soluble ("streaking") isolated band. Thus, a mixture of both the nickel(II) *cis*- (5) and *trans*-dimer (7) was apparent.

The fast running compound was tentatively assigned the *cis*-configuration (5) due to its optical similarity to the copper(II) *cis*-compound (4) as well as with the 1,2-phenylene-bridged bisporphyrin described by Osuka et al.<sup>8e</sup> This assignment was subsequently confirmed by spectroscopic and X-ray crystallographic means. A variable temperature (VT) proton NMR study (Figure 1) was conducted on a fraction which contained the two isomers in approximately equal amounts. Utilizing [D<sub>2</sub>]-1,1,2,2-tetrachloroethane as solvent, the temperature was varied from 25 to 140 °C. As the temperature increased the peaks at 9.30, 9.05, and 8.06 ppm decreased relative to those at 9.50, 9.48, and 7.66 ppm which also broadened at higher temperatures (>100 °C) (Figure 1B,C). Heating at 120 °C in the dark, overnight converted the mixture into a single isomer (Figure 1E); proton NMR data confirmed this observation. These data indicated isomerization of the *cis*-compound to the thermodynamically favored *trans*-derivative in the slightly acidic tetrachloroethane. Refluxing acidic (H<sub>2</sub>SO<sub>4</sub>) THF, however, did not promote isomerization, indicating a large thermal barrier for isomerization.

In order to unequivocally assign the structure of the individual isomers, the *trans*-isomer was prepared using the method of Shul'ga and Ponomarev.<sup>17</sup> Following this method Cu(II) 5-formyl-OEP (2) was reduced in the presence of NaBH<sub>4</sub> to give the 5-hydroxymethyl-OEP derivative (8). Self-condensation to the ethane-bridged bis-porphyrin (9) was easily accomplished with TFA. Demetallation to the free-base dimer (10) was required to oxidize the ethane-bisporphyrin to the *trans*-ethene-bisporphyrin (11). Although the mechanism is still unclear, it was shown recently that the oxidation proceeds through an intermediate with monoprotonated OEP.<sup>18</sup> Metalation of 11 with Ni(acac)<sub>2</sub> gave the nickel *trans*-ethene-bridged dimer 7. When the free base dimer 11 was metalated with copper(II), the product (6) was insoluble in most organic solvents. It now appears likely that 6 was produced in the low valent titanium coupling but was lost on the column due to its insolubility.

Table 1. Crystallographic Data for Compounds 4, 5, 7, and 13

	compound			
	4	5	7	13
chem formula	C <sub>74</sub> H <sub>87</sub> Cu <sub>2</sub> N <sub>8</sub>	C <sub>74</sub> H <sub>87</sub> N <sub>8</sub> Ni <sub>2</sub>	C <sub>74</sub> H <sub>87</sub> N <sub>8</sub> Ni <sub>2</sub> -C <sub>7</sub> H <sub>8</sub>	C <sub>69</sub> H <sub>80</sub> N <sub>8</sub> Ni <sub>2</sub> O-CH <sub>2</sub> Cl <sub>2</sub>
mol wt	1216.6	1206.9	1323.1	1154.3
cryst shape	blue parallelepiped	black parallelepiped	black parallelepiped	red parallelepiped
cryst size, mm	0.52 × 0.32 × 0.21	0.5 × 0.2 × 0.18	0.22 × 0.15 × 0.03	0.35 × 0.22 × 0.11
space group	P2 <sub>1</sub> /n	P2 <sub>1</sub> /c	P1	C2/c
a, Å	19.208(7)	21.671(7)	11.163(3)	40.31(2)
b, Å	14.672(5)	14.079(4)	12.775(4)	14.997(7)
c, Å	24.170(7)	22.110(7)	14.554(3)	21.954(11)
α, deg	90	90	69.59(2)	90
β, deg	111.15(3)	108.86(2)	81.15(2)	108.6(4)
γ, deg	90	90	73.21(2)	90
V, Å <sup>3</sup>	6352(4)	6384(3)	1859(1)	12579(10)
Z	4	4	1	8
D <sub>calcd</sub> , g cm <sup>-3</sup>	1.271	1.256	1.182	1.219
μ(Mo Kα), mm <sup>-1</sup>	0.718	0.639	0.991 (Cu Kα)	0.735
λ, Å	0.710 69	0.710 69	1.541 78	0.710 69
2θ <sub>max</sub> , deg	55	55	112	48
no. of ind reflns	14 681	14 663	4835	7929
no. of obsd reflns	8040 (F > 5σ(F))	8909 (F > 3σ(F))	3790 (F > 4σ(F))	5146 (F > 2σ(F))
no. of variables	755	757	442	549
T, K	130	130	126	130
R	0.056	0.064	0.072	0.122
wR	0.064	0.075	0.097	0.120
S	1.22	0.97	1.21	1.45

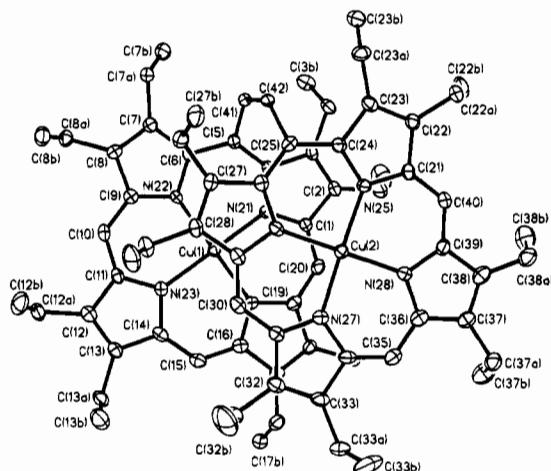


Figure 4. Computer-generated plot and numbering scheme of the copper *cis*-dimer, 4. Ellipsoids are drawn for 50% occupancy; hydrogen atoms have been omitted for clarity.

The UV/vis spectrum of the nickel dimer prepared by the method of Ponomarev and co-workers<sup>17</sup> matched that from the less-soluble product of the titanium coupling reaction; proton-NMR data also confirmed the correct assignment of this fraction as the *trans*-isomer (7) (Figure 3A). As mentioned above, separation of the two nickel isomers using column chromatography was very difficult but successful using fractional crystallization. The *trans*-isomer (7) was much less soluble than the *cis*-isomer (5) in most organic solvents. The *cis*-isomer (5) was easily extracted from the *trans*-isomer (7) using appropriate solvents with the *trans*-isomer remaining as a solid.

Crystals were grown of each isomer and subsequent single crystal X-ray structure determination (see below) confirmed the above structural assignments. Concurrent work by Ponomarev and co-workers<sup>19</sup> led also to synthesis of the *cis*- and *trans*-nickel dimers. They developed an isomerization of the free base *trans*-ethene-OEP (11) to the *cis*-isomer in the presence of refluxing glacial acetic acid. After metalation of both isomers with Ni(OAc)<sub>2</sub> they derived structural conclusions similar to our own. Their conclusions were initially based on NOE experiments, and recently X-ray crystallographic data were presented for the Ni(II) *trans*-dimer.<sup>19b</sup>

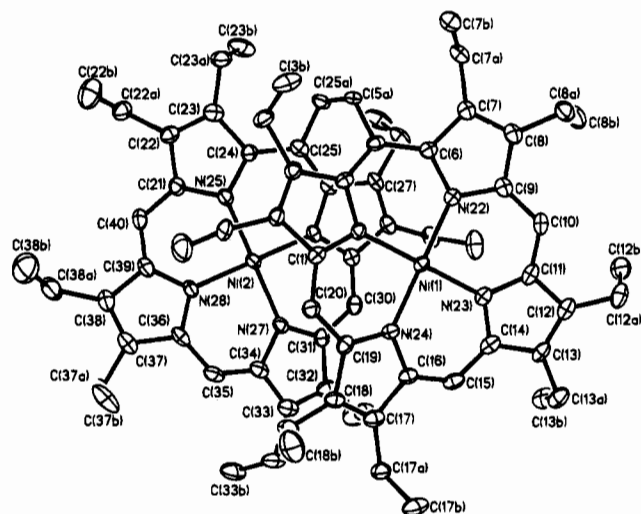


Figure 5. Computer generated plot and numbering scheme of the nickel *cis*-dimer, 5. Ellipsoids are drawn for 50% occupancy; hydrogen atoms have been omitted for clarity.

The *trans*-isomer is usually the observed product in carbonyl coupling reactions of formyl-substituted organic substrates.<sup>10b</sup> Previous work on porphyrins<sup>11</sup> utilizing the McMurry reaction has yielded *trans*-products, as did work on bispyrroles.<sup>20</sup> For a bisporphyrin with a stilbene linkage this was proven by a X-ray structure analysis.<sup>21</sup> It is possible that porphyrin aggregation effects *prior* to coupling may force the macrocycles in close proximity to each other, with attractive effects outweighing any steric interactions, leading to the *cis*-products. Alternatively it is possible that steric effects of the porphyrin rings with the titanium surface direct the stereochemistry forcing the molecule into the *cis*-conformation during the reaction.

It should also be noted that reductive coupling of  $\beta$ -formyl OEP (12) leads again not to the anticipated product, a 1,2-bis-[2-(3,7,8,12,13,17,18-heptaethylporphyrinato)nickel(II)]-ethene, but rather yields bis[2-(3,7,8,12,13,17,18-heptaethylporphyrinato)nickel(II)]hydroxymethane (13), with loss of a one

(20) Wallace, D. M. Ph.D. Dissertation, University of California, Davis, 1992.

(21) Gerzevske, K. R.; Senge, M. O.; Smith, K. M. Unpublished results.

**Table 2.** Atomic Coordinates and Isotropic Temperature Factors ( $\text{\AA}^2$ ) for 1,2-Bis[5-(2,3,7,8,12,13,17,18-octaethylporphyrinato)copper(II)]*cis*-ethene, **4**

atom	x	y	z	$U(\text{eq})^a$	atom	x	y	z	$U(\text{eq})^a$
Cu(1)	9723(1)	4927(1)	914(1)	15(1)	N(25)	8370(2)	6193(2)	2436(1)	16(1)
N(21)	9594(2)	6076(2)	1307(1)	16(1)	N(26)	8414(2)	4746(2)	1690(1)	19(1)
N(22)	8944(2)	5363(2)	162(1)	14(1)	N(27)	9526(2)	3876(2)	2666(1)	18(1)
N(23)	9840(2)	3771(2)	519(1)	17(1)	N(28)	9568(2)	5393(2)	3383(1)	20(1)
N(24)	10503(2)	4501(2)	1668(1)	16(1)	C(21)	8435(3)	6832(3)	2868(2)	20(2)
C(1)	10038(2)	6370(3)	1863(1)	18(2)	C(22)	7877(3)	7529(3)	2648(2)	21(2)
C(2)	9774(3)	7234(3)	1995(2)	22(2)	C(22A)	7783(3)	8346(3)	2990(2)	27(2)
C(2A)	10120(3)	7788(3)	2552(2)	36(2)	C(22B)	8313(3)	9116(3)	2995(2)	36(2)
C(2B)	10606(3)	8556(4)	2474(3)	59(3)	C(23)	7457(2)	7313(3)	2071(2)	21(2)
C(3)	9135(2)	7436(2)	1526(2)	18(2)	C(23A)	6720(2)	7753(3)	1723(2)	27(2)
C(3A)	8701(2)	8309(2)	1458(2)	22(2)	C(23B)	6749(3)	8660(3)	1430(2)	34(2)
C(3B)	8781(3)	8931(3)	982(2)	32(2)	C(24)	7803(2)	6500(3)	1938(2)	18(2)
C(4)	9020(2)	6694(3)	1101(2)	16(1)	C(25)	7640(2)	6120(3)	1371(2)	17(2)
C(5)	8415(2)	6608(3)	560(2)	17(1)	C(26)	7870(2)	5250(3)	1272(2)	18(1)
C(6)	8433(2)	6051(2)	91(2)	17(2)	C(27)	7570(2)	4736(3)	718(2)	18(2)
C(7)	7917(2)	6084(3)	-526(2)	18(2)	C(27A)	6870(2)	4938(3)	195(2)	23(2)
C(7A)	7280(2)	6728(2)	-819(2)	22(2)	C(27B)	6172(2)	4878(3)	349(2)	31(2)
C(7B)	7532(3)	7690(3)	-883(2)	30(2)	C(28)	7965(2)	3951(3)	800(2)	20(2)
C(8)	8148(2)	5428(3)	-817(1)	17(1)	C(28A)	7882(3)	3184(3)	367(2)	28(2)
C(8A)	7800(2)	5174(3)	-1462(1)	22(2)	C(28B)	7334(3)	2451(3)	387(2)	42(2)
C(8B)	7153(2)	4514(3)	-1577(2)	29(2)	C(29)	8481(2)	3955(2)	1407(2)	19(2)
C(9)	8764(2)	4957(3)	-385(1)	16(1)	C(30)	8947(3)	3239(3)	1673(2)	21(2)
C(10)	9048(2)	4140(3)	-493(2)	18(2)	C(31)	9405(2)	3175(2)	2264(2)	19(2)
C(11)	9524(2)	3570(3)	-75(1)	17(2)	C(32)	9826(3)	2381(3)	2537(2)	23(2)
C(12)	9722(2)	2653(3)	-181(2)	21(2)	C(32A)	9787(3)	1473(3)	2238(2)	35(2)
C(12A)	9423(2)	2177(3)	-771(2)	28(2)	C(32B)	9113(3)	916(4)	2218(3)	63(3)
C(12B)	8660(2)	1763(4)	-882(2)	41(2)	C(33)	10212(2)	2595(3)	3110(2)	24(2)
C(13)	10166(2)	2307(2)	345(2)	20(2)	C(33A)	10969(2)	1996(3)	3604(2)	33(2)
C(13A)	10510(2)	1373(2)	474(2)	25(2)	C(33B)	10298(3)	1610(4)	3992(2)	52(3)
C(13B)	10061(1)	689(2)	680(1)	39(2)	C(34)	10030(2)	3534(3)	3187(2)	22(2)
C(14)	10248(1)	3014(2)	781(1)	19(2)	C(35)	10325(3)	4024(3)	3708(2)	25(2)
C(15)	10688(1)	2952(2)	1378(1)	21(2)	C(36)	10120(2)	4900(3)	3801(2)	24(2)
C(16)	10822(2)	3650(2)	1790(2)	19(2)	C(37)	10403(2)	5363(3)	4365(2)	24(2)
C(17)	11332(2)	3604(3)	2396(2)	21(2)	C(37A)	11015(2)	5026(3)	4915(2)	29(2)
C(17A)	11777(2)	2776(3)	2685(2)	25(2)	C(37B)	11785(2)	5260(4)	4916(2)	44(2)
C(17B)	12499(2)	2661(3)	2570(2)	27(2)	C(38)	10005(3)	6160(3)	4290(2)	27(2)
C(18)	11348(2)	4433(3)	2634(2)	20(2)	C(38A)	10064(3)	6903(3)	4733(2)	33(2)
C(18A)	11821(2)	4768(3)	3242(2)	28(2)	C(38B)	10481(3)	7727(3)	4634(3)	47(2)
C(18B)	12518(2)	5259(3)	3245(2)	35(2)	C(39)	9488(3)	6161(3)	3680(2)	23(2)
C(19)	10815(2)	4997(3)	2182(1)	21(1)	C(40)	8957(3)	6823(3)	3439(2)	23(2)
C(20)	10619(2)	5870(3)	2258(2)	21(2)	C(41)	7687(2)	7019(3)	514(2)	17(2)
Cu(2)	8989(1)	5068(1)	2536(1)	17(1)	C(42)	7324(2)	6754(3)	860(2)	17(1)

<sup>a</sup> Equivalent isotropic  $U$  defined as one-third of the trace of the orthogonalized  $U_{ij}$  tensor.

carbon unit.<sup>11b</sup> The mechanism for the formation of **13** is still unknown; however, steric effects may play a role. It can be speculated that after reductive addition to the Ti surface, the porphyrins may be situated to favor a concerted C–O elimination of one of the porphyrins with simultaneous radical coupling of the  $\beta$ -free porphyrin with the hydroxymethyl of the other porphyrin before elimination from the titanium surface.

**Structural Studies.** Structure of 1,2-Bis[5-(2,3,7,8,12,13,17,18-octaethylporphyrinato)copper(II)]-*cis*-ethene, **4**. The molecular structure of **4** is shown in Figure 4. Atomic coordinates are listed in Table 2, while selected bond lengths and angles are compiled in Table 6. The structure clearly shows the *cis*-arrangement about the connecting ethene bridge ( $-\text{CH}=\text{CH}-$  distance 1.327(7)  $\text{\AA}$ ). The most intriguing feature of this type of face-to-face structures is the almost coplanar arrangement of the two porphyrin macrocycles. The angle between the two four nitrogen planes (4N-plane) is only 1.9°. This can only be explained by  $\pi$ - $\pi$ -interaction between the two porphyrin macrocycles. If no aggregation were present the geometry at the connecting double bond would require angles of 60°.

The strong overlap of the  $\pi$ -systems is shown in Figure 6. Scheidt and Lee have suggested a classification system for such dimers.<sup>22</sup> Accordingly the most important geometrical features of an aggregate dimer are the mean separation of the macrocycle

plane (we used the 4N-planes) and the lateral shift of the centers.<sup>23</sup> In the copper *cis*-ethene dimer (**4**) the two copper atoms are separated by 4.626  $\text{\AA}$  and the center-to-center distance is 4.661  $\text{\AA}$ . The two 4N-planes are spaced 3.358  $\text{\AA}$  apart and the slip angle is 43.9°. These values give a lateral shift of the centers of 3.232  $\text{\AA}$ . Thus the present intramolecular aggregate falls into the middle range of this type of aggregation as classified by Scheidt and Lee.<sup>22</sup> With their cofacial structure, electronic coupling as evidenced by the UV/vis and the small interplanar separation, these compounds are promising model compounds for the special pair in photosynthesis. Note that the interplanar distance in the special pair of *Rhodospseudomonas viridis* is about 3.3  $\text{\AA}$ ,<sup>4a</sup> which compares well with a spacing of 3.36  $\text{\AA}$  found in the copper dimer **4**. A correct interplanar spacing is one of the crucial features of a special pair model compound. A recent theoretical examination of the electronic structure and excited states of the bacteriochlorophyll b dimer in *R. viridis* showed that the lowest  $Q_y$  band is blue shifted by an increase in the macrocycle spacing.<sup>24</sup> Nevertheless, the described compounds present only a first step towards the

(22) Scheidt, W. R.; Lee, Y. J. *Struct. Bonding (Berlin)* **1987**, *64*, 1.

(23) The center of a macrocycle is defined here as the geometrical center of the 4N-plane. The lateral shift is defined as  $L.S. = \{\sin(\text{slip angle}) \times \text{center-to-center distance}\}$ .<sup>22</sup> The slip angle is the angle formed between the center-to-center vector and the 4N-planes of the macrocycles.

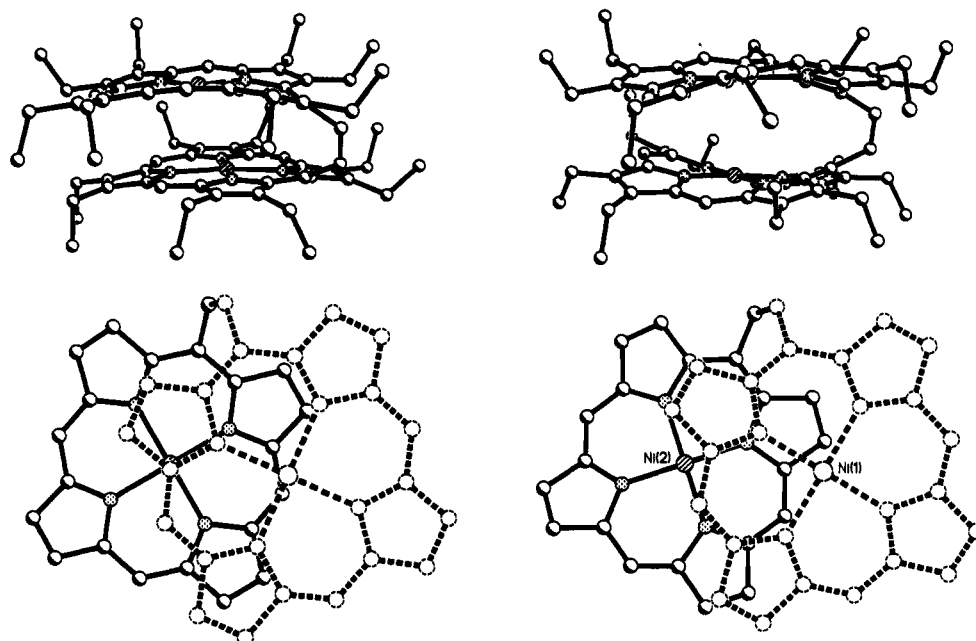


**Figure 6.** Side views (top row) of the copper (left panel) and nickel (right panel) *cis*-dimers, **4** and **5**. The bottom row shows a top view of the macrocycle overlap in the respective dimers. The paper plane is the 4N-plane of the upper (dashed) macrocycle.

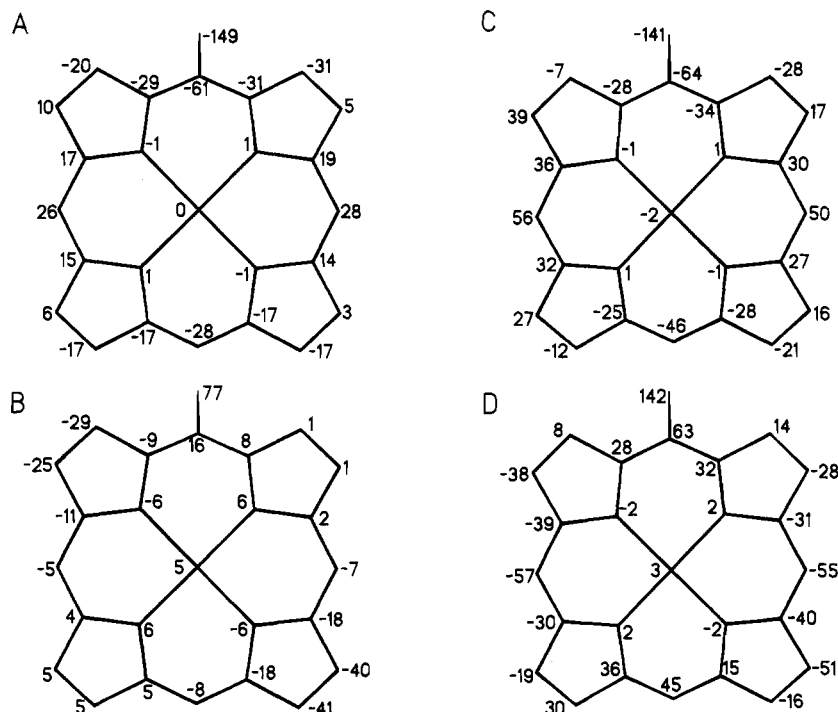


**Figure 7.** Deviations from the least-squares 4N-plane for the copper dimer, **4** (A, B) and the nickel dimer, **5** (C, D) [ $\text{\AA} \times 10^2$ ].

synthesis of true models for the photosynthetic reaction center, which requires different metals and more complex ligand systems.

This coplanar arrangement of the macrocycles is similar to that observed for e.g. biphenylene bridged bis-porphyrins and related compounds. However, it should be noted that the cofacial structure observed here is obtained not by attaching two porphyrin macrocycles onto a rigid bridging unit, like 1,2-phenylene,<sup>8g</sup> which forces the macrocycles into a face-to-face arrangement. Instead the present synthetic methodology is based on bridging the porphyrins with a small (variable) linker which allows the formation of either extended, linear, or skewed or cofacial structures. The observation of the coplanar face-to-

face structure is therefore due to aggregation and not geometrical constraints imposed on the systems by the choice of the bridging unit.

The geometry of the present dimer agrees well with the predictions made first by Abraham et al. for the aggregation of (monomeric) metalloporphyrins on the basis of NMR.<sup>25</sup> Similar results were obtained using EPR measurements<sup>26</sup> and other work of Hunter and Sanders.<sup>27</sup> Recently we were able to confirm the model developed by Abraham et al. for the situation in

(24) Thompson, M. A.; Zemer, M. C.; Fajer, J. *J. Phys. Chem.* **1991**, *95*, 5693.

(25) (a) Abraham, R. J.; Eivazi, F.; Pearson, H.; Smith, K. M. *J. Chem. Soc., Chem. Commun.* **1976**, 698. (b) *Ibid.*, p 699. (c) Abraham, R. J.; Barnett, G. H.; Hawkes, G. E.; Smith, K. M. *Tetrahedron* **1976**, *32*, 2949. Abraham, R. J.; Evans, B.; Smith, K. M. *Tetrahedron* **1978**, *34*, 1213. Abraham, R. J.; Fell, S. C. M.; Pearson, H.; Smith, K. M. *Tetrahedron* **1979**, *35*, 1759. (d) Snyder, R. V.; La Mar, G. N. *J. Am. Chem. Soc.* **1977**, *99*, 7178.

**Table 3.** Atomic Coordinates and Isotropic Temperature Factors ( $\text{\AA}^2$ ) for 1,2-Bis[5-(2,3,7,8,12,13,17,18-octaethylporphyrinato)nickel(II)]-*cis*-ethene, **5**

	x	y	z	U(eq) <sup>a</sup>		x	y	z	U(eq) <sup>a</sup>
Ni(1)	1252(1)	295(1)	25(1)	21(1)	Ni(2)	3626(1)	468(1)	82(1)	23(1)
N(21)	1987(2)	-474(2)	478(2)	22(1)	N(25)	3962(2)	-789(3)	33(2)	27(1)
N(22)	844(2)	-829(2)	-431(2)	23(1)	N(26)	2862(2)	149(3)	-603(2)	24(1)
N(23)	508(2)	1063(3)	-423(2)	25(1)	N(27)	3310(2)	1752(3)	98(2)	25(1)
N(24)	1656(2)	1410(2)	502(2)	23(1)	N(28)	4401(2)	785(3)	768(2)	28(1)
C(1)	2455(2)	-244(3)	1051(2)	26(2)	C(21)	4604(2)	-1065(3)	286(2)	28(2)
C(2)	2891(2)	-1027(3)	1285(2)	27(2)	C(22)	4682(2)	-2039(3)	126(2)	29(2)
C(2A)	3426(2)	-1024(3)	1930(2)	39(2)	C(22A)	5323(2)	-2545(3)	283(2)	37(2)
C(2B)	4056(3)	-620(4)	1901(3)	58(2)	C(22B)	5527(3)	-3078(5)	916(3)	64(3)
C(3)	2726(2)	-1712(3)	831(2)	26(2)	C(23)	4078(2)	-2390(3)	-188(2)	32(2)
C(3A)	3033(2)	-2685(3)	924(2)	33(2)	C(23A)	3958(3)	-3376(3)	-460(3)	41(2)
C(3B)	2624(3)	-3408(3)	1140(3)	47(2)	C(23B)	3843(3)	-3415(4)	-1177(3)	56(3)
C(4)	2154(2)	-1369(3)	335(2)	23(1)	C(24)	3623(2)	-1590(3)	-259(2)	26(2)
C(5)	1785(2)	-1892(3)	-200(2)	25(2)	C(25)	2960(2)	-1590(3)	-601(2)	27(2)
C(5A)	2096(2)	-2652(3)	-463(2)	28(2)	C(25A)	2601(2)	-2499(3)	-674(2)	29(2)
C(6)	1130(2)	-1683(3)	-513(2)	24(1)	C(26)	2637(2)	-742(3)	-829(2)	24(2)
C(7)	640(2)	-2301(3)	-939(2)	28(2)	C(27)	2046(2)	-670(3)	-1380(2)	29(2)
C(7A)	708(2)	-3308(3)	-1137(2)	37(2)	C(27A)	1714(3)	-1424(3)	-1852(2)	39(2)
C(7B)	747(3)	-4035(3)	-613(3)	44(2)	C(27B)	2089(3)	-1608(4)	-2314(3)	58(3)
C(8)	63(2)	-1832(3)	-1080(2)	30(2)	C(28)	1924(2)	274(3)	-1485(2)	29(2)
C(8A)	-594(2)	-2140(4)	-1517(2)	38(2)	C(28A)	1384(2)	729(4)	-2019(2)	36(2)
C(8B)	-717(3)	-1808(4)	-2203(2)	47(2)	C(28B)	737(3)	771(5)	-1894(2)	52(2)
C(9)	198(2)	-919(3)	-783(2)	26(2)	C(29)	2416(2)	777(3)	-992(2)	26(2)
C(10)	-252(2)	-194(3)	-917(2)	29(2)	C(30)	2413(2)	1746(3)	-898(2)	30(2)
C(11)	-93(2)	746(3)	-783(2)	26(2)	C(31)	2828(2)	2209(3)	-379(2)	27(2)
C(12)	-528(2)	1521(3)	-1055(2)	31(2)	C(32)	2798(2)	3208(3)	-235(2)	32(2)
C(12A)	-1210(2)	1407(4)	-1498(2)	42(2)	C(32A)	2344(3)	3909(4)	-658(3)	45(2)
C(12B)	-1240(3)	1199(4)	-2187(2)	47(2)	C(32B)	2592(3)	4346(4)	-1158(3)	60(3)
C(13)	-179(2)	2332(3)	-869(2)	30(2)	C(33)	3255(2)	3335(3)	347(2)	34(2)
C(13A)	-379(3)	3343(3)	-1034(2)	41(2)	C(33A)	3448(3)	4261(3)	706(3)	42(2)
C(13B)	-153(3)	3735(4)	-1566(2)	47(2)	C(33B)	4096(3)	4655(4)	682(3)	52(2)
C(14)	462(2)	2044(3)	-458(2)	29(2)	C(34)	3569(2)	2448(3)	554(2)	28(2)
C(15)	936(2)	2650(3)	-106(2)	30(2)	C(35)	4086(2)	2304(3)	1095(2)	32(2)
C(16)	1484(2)	2345(3)	372(2)	26(2)	C(36)	4488(2)	1541(3)	1190(2)	30(2)
C(17)	1911(2)	2963(3)	849(2)	31(2)	C(37)	5131(2)	1499(4)	1659(2)	38(2)
C(17A)	1870(2)	4025(3)	857(2)	34(2)	C(37A)	5377(3)	2148(4)	2228(2)	45(2)
C(17B)	1387(3)	4409(3)	1157(3)	45(2)	C(37B)	5088(3)	1928(5)	2749(3)	66(3)
C(18)	2331(2)	2389(3)	1287(2)	26(2)	C(38)	5449(2)	781(4)	1489(2)	36(2)
C(18A)	2855(2)	2648(3)	1889(2)	33(2)	C(38A)	6149(3)	472(4)	1790(3)	52(2)
C(18B)	2664(3)	2547(5)	2478(2)	58(2)	C(38B)	6237(4)	-205(5)	2323(3)	79(3)
C(19)	2176(2)	1428(3)	1057(2)	25(2)	C(39)	4985(2)	316(3)	951(2)	32(2)
C(20)	2530(2)	639(3)	1333(2)	28(2)	C(40)	5090(2)	-536(3)	697(2)	34(2)

<sup>a</sup> Equivalent isotropic  $U$  defined as one-third of the trace of the orthogonalized  $U_{ij}$  tensor.

solution with X-ray crystallography for the solid state.<sup>28</sup> In both cases the (mono)metalloporphyrins aggregate by forming coplanar arrangements spaced about 3–4 Å apart. The macrocycles do not completely overlap but rather show a sideways displacement with a lateral shift of 3–5 Å.<sup>25</sup> If asymmetric porphyrins with e.g. one *meso*-substituent were used, then aggregation led to the formation of head-to-tail structures to minimize steric interactions of the *meso*-substituents. A similar situation is found in the present structure with its coplanar macrocycles and sideways displacement of the rings. A complete overlap of the  $\pi$ -systems is thus not to be expected. However, there are several examples in the literature where more overlap of the  $\pi$ -systems and stronger aggregation (indicated by smaller interplanar distances) was observed for (mono)porphyrins.<sup>22</sup> These include  $\pi$ -cation radicals,<sup>29</sup> asymmetric substituted metalloporphyrins,<sup>28</sup> and other species.<sup>30</sup>

The only discrepancy with the earlier work involves the orientation of the connecting positions. One of the requirements noted was that the macrocycle has to be asymmetric.<sup>25a,b,28</sup> By

necessity the present structure is of the head-to-head type, i.e. the two *meso*-substituted positions point into the same direction. Here the connecting bridge forces the macrocycles so close to each other that steric considerations have been overcome already and (further) aggregation is the only course of action. In any case, the requirement for head-to-tail arrangement seems not to be a strict one. Several examples of symmetric metalloporphyrins have been described in the literature which show moderate aggregation.<sup>26,27,30–32</sup>

The geometry of the core of the porphyrins units in **4** resembles closely the situation found in related (monomeric) copper(II) porphyrins. The average length of the Cu–N bond is 1.998(2) Å; this agrees well with the data found in Cu<sup>II</sup>-OEP<sup>32b,33</sup> and is slightly longer than distances found in Cu<sup>II</sup>-

- (26) Blumberg, W. E.; Peisach, J. *J. Biol. Chem.* **1965**, *240*, 870. Boas, J. F.; Pilbrow, J. R.; Smith, T. D. *J. Chem. Soc. A* **1969**, 721. Chikira, M.; Kon, H.; Smith, K. M. *J. Chem. Soc., Chem. Commun.* **1978**, 906; *J. Chem. Soc., Dalton Trans.* **1980**, 526; **1981**, 1726.  
 (27) Hunter, C. A.; Sanders, J. K. M. *J. Am. Chem. Soc.* **1990**, *112*, 5525.  
 (28) Senge, M. O.; Eigenbrot, C. W.; Brennan, T. D.; Shusta, J.; Scheidt, W. R.; Smith, K. M. *Inorg. Chem.* **1993**, *32*, 3134.

- (29) Scheidt, W. R.; Lee, Y. J.; Hatano, K. *J. Am. Chem. Soc.* **1984**, *106*, 3191. Scheidt, W. R.; Geiger, D. K.; Lee, Y. J.; Reed, C. A.; Lang, G. *J. Am. Chem. Soc.* **1985**, *107*, 5693. Song, H.; Reed, C. A.; Scheidt, W. R. *J. Am. Chem. Soc.* **1989**, *111*, 6867. Song, H.; Orosz, R. D.; Reed, C. A.; Scheidt, W. R. *Inorg. Chem.* **1990**, *29*, 4274. Scheidt, W. R.; Song, H.; Haller, K. J.; Safo, M. K.; Orosz, R. D.; Reed, C. A.; Debrunner, P. G.; Schulz, C. E. *Inorg. Chem.* **1992**, *31*, 939.  
 (30) For a complete listing see ref 22.  
 (31) Senge, M. O.; Smith, K. M. *Z. Naturforsch.* **1993**, *48b*, 991.  
 (32) (a) Alden, R. G.; Ondrias, M. R.; Shelnuitt, J. A. *J. Am. Chem. Soc.* **1990**, *112*, 691. (b) Sparks, L. D.; Scheidt, W. R.; Shelnuitt, J. A. *Inorg. Chem.* **1992**, *31*, 2191.  
 (33) Pak, R.; Scheidt, W. R. *Acta Crystallogr., Part C* **1991**, *47*, 431.



**Table 4.** Selected Atomic Coordinates and Isotropic Temperature Factors ( $\text{\AA}^2$ ) for 1,2-Bis[5-(2,3,7,8,12,13,17,18-octaethylporphyrinato)nickel(II)]-*trans*-ethene, **7**

	x	y	z	$U(\text{eq})^a$
Ni	1762(1)	696(1)	773(1)	13(1)
N(21)	1135(3)	1587(3)	1643(3)	16(2)
N(22)	567(3)	1755(3)	-136(3)	14(2)
N(23)	2377(4)	-213(3)	-91(3)	15(2)
N(24)	2955(4)	-381(3)	1701(3)	16(2)
C(1)	1294(4)	1230(4)	2637(3)	16(2)
C(2)	671(4)	2129(4)	3046(3)	16(2)
C(21)	578(5)	2017(4)	4110(4)	22(2)
C(22)	-570(6)	1619(5)	4664(4)	35(3)
C(3)	184(4)	3083(4)	2286(3)	15(2)
C(31)	-634(5)	4205(4)	2391(4)	22(2)
C(32)	-2022(5)	4257(4)	2449(4)	25(2)
C(4)	453(4)	2740(4)	1404(4)	15(2)
C(5)	0(4)	3389(4)	491(3)	14(2)
C(51)	-395(5)	4682(4)	216(3)	16(2)
C(6)	-78(4)	2886(4)	-198(3)	16(2)
C(7)	-913(4)	3387(4)	-1004(3)	16(2)
C(71)	-1891(4)	4520(4)	-1262(4)	19(2)
C(72)	-3078(5)	4430(5)	-581(4)	28(2)
C(8)	-788(4)	2539(4)	-1411(3)	15(2)
C(81)	-1416(5)	2621(4)	-2275(4)	24(2)
C(82)	-641(6)	2996(5)	-3241(4)	34(2)
C(9)	153(4)	1558(4)	-896(3)	15(2)
C(10)	674(4)	607(4)	-1194(3)	14(2)
C(11)	1771(4)	-200(4)	-851(3)	15(2)
C(12)	2507(4)	-1039(4)	-1305(3)	16(2)
C(121)	2120(5)	-1261(5)	-2150(4)	25(2)
C(122)	2436(6)	-448(6)	-3156(4)	38(3)
C(13)	3604(5)	-1514(4)	-852(4)	19(2)
C(131)	4724(5)	-2406(4)	-1074(4)	22(2)
C(132)	5758(5)	-1873(5)	-1704(5)	36(3)
C(14)	3504(4)	-1047(4)	-75(3)	15(2)
C(15)	4306(5)	-1441(4)	667(4)	18(2)
C(16)	4009(4)	-1183(4)	1530(3)	17(2)
C(17)	4662(5)	-1830(4)	2425(4)	17(2)
C(171)	5866(4)	-2745(4)	2501(4)	21(2)
C(172)	7005(5)	-2246(5)	2132(4)	32(2)
C(18)	3950(4)	-1459(4)	3155(3)	18(2)
C(181)	4178(5)	-1848(4)	4223(4)	23(2)
C(182)	4827(6)	-1103(5)	4486(4)	34(3)
C(19)	2908(4)	-525(4)	2686(3)	15(2)
C(20)	2076(4)	193(4)	3139(3)	16(2)

<sup>a</sup> Equivalent isotropic  $U$  defined as one-third of the trace of the orthogonalized  $U_{ij}$  tensor.

TPP<sup>34</sup> or Cu(II) octaethyltetraphenylporphyrin.<sup>35</sup> The general trends in bond lengths and angles of the core, macrocycle and side chains agree well with those observed in related systems.<sup>22</sup>

A conformational analysis of the two macrocycles (Figure 7A,B) shows that the two ring systems are not equivalent. The porphyrin ring with Cu(1) (Figure 7A) has a mean deviation from planarity of 0.226  $\text{\AA}$ , the ring with Cu(2) of 0.137  $\text{\AA}$ . The individual pyrrole rings are rotated on average by 10.8° against the 4N-plane in macrocycle 1 and 4.1° in macrocycle 2. The average deviation of the *meso*-carbons from the 4N-plane is 0.36  $\text{\AA}$  in macrocycle 1 and 0.09  $\text{\AA}$  in macrocycle 2. The individual displacement of the *meso*-carbons is however strongly inequivalent in ring 1. While the unsubstituted *meso*-carbons [C(10), C(15), and C(20)] are displaced evenly by 0.28  $\text{\AA}$  the carbon atom bearing the connecting ethene group is displaced by 0.61  $\text{\AA}$ . A similar tendency also less pronounced is observed in ring 2 with values of 0.16  $\text{\AA}$  versus 0.07  $\text{\AA}$ . This inequivalence is explained by the local distortion induced by the *meso*-substituent being flanked by two ethyl groups in close proximity.

(34) Fleischer, E. B.; Miller, C. K.; Webb, L. E. *J. Am. Chem. Soc.* **1964**, *86*, 2342.

(35) Sparks, L. D.; Medforth, C. J.; Park, M.-S.; Chamberlain, J. R.; Ondrias, M. R.; Senge, M. O.; Smith, K. M.; Shelnutt, J. A. *J. Am. Chem. Soc.* **1993**, *115*, 581.

**Table 5.** Selected Atomic Coordinates and Isotropic Temperature Factors ( $\text{\AA}^2$ ) for 1,1-Bis[2-(3,7,8,12,13,17,18-heptaethylporphyrinato)nickel(II)]carbinol, **13**

atom	x	y	z	$U(\text{eq})^a$
Ni(1)	143(1)	594(1)	4037(1)	28(1)
N(21)	135(2)	1868(2)	3853(4)	31(4)
N(22)	500(2)	781(5)	4870(2)	28(4)
N(23)	144(3)	-681(2)	4219(4)	32(5)
N(24)	-202(2)	409(5)	3191(2)	27(4)
C(1)	-106(3)	2321(7)	3353(5)	30(3)
C(2)	-20(3)	3276(8)	3429(6)	37(3)
C(3)	271(3)	3380(8)	3931(7)	44(4)
C(4)	368(3)	2494(7)	4219(6)	35(3)
C(5)	632(3)	2335(8)	4765(6)	28(3)
C(6)	688(3)	1555(6)	5097(6)	28(3)
C(7)	924(3)	1404(8)	5743(6)	30(3)
C(8)	868(3)	575(8)	5928(5)	40(4)
C(9)	604(3)	184(7)	5379(5)	30(3)
C(10)	508(3)	-697(8)	5342(6)	31(3)
C(11)	303(3)	-1113(7)	4799(4)	26(3)
C(12)	247(3)	-2069(8)	4722(6)	33(3)
C(13)	63(4)	-2230(9)	4098(7)	46(4)
C(14)	-17(3)	-1353(7)	3792(6)	38(4)
C(15)	-218(4)	-1216(9)	3163(7)	45(4)
C(16)	-307(3)	-393(6)	2872(6)	31(3)
C(17)	-546(3)	-250(7)	2245(6)	28(3)
C(18)	-606(3)	639(8)	2181(5)	32(3)
C(19)	-391(3)	1042(6)	2758(5)	26(3)
C(20)	-352(3)	1933(8)	2864(6)	31(3)
Ni(2)	1963(1)	3252(1)	4654(1)	23(1)
N(25)	1674(2)	3230(5)	5219(4)	28(4)
N(26)	1936(3)	4552(2)	4618(4)	25(4)
N(27)	2244(2)	3270(5)	4077(4)	23(4)
N(28)	1986(2)	1952(2)	4675(4)	22(4)
C(21)	1538(2)	2489(6)	5435(6)	24(3)
C(22)	1329(3)	2764(8)	5822(6)	30(3)
C(23)	1334(3)	3669(8)	5860(6)	32(3)
C(24)	1543(3)	3955(7)	5464(6)	39(4)
C(25)	1604(3)	4845(9)	5343(7)	38(4)
C(26)	1781(3)	5129(7)	4943(6)	35(4)
C(27)	1812(3)	6031(7)	4790(6)	29(3)
C(28)	1986(3)	6060(7)	4357(6)	28(3)
C(29)	2068(3)	5124(7)	4254(6)	29(3)
C(30)	2250(3)	4858(8)	3862(6)	31(3)
C(31)	2339(3)	3998(6)	3777(5)	22(3)
C(32)	2535(3)	3724(7)	3358(6)	30(3)
C(33)	2574(3)	2835(7)	3417(5)	22(3)
C(34)	2389(3)	2547(6)	3856(6)	26(3)
C(35)	2356(3)	1677(8)	4019(6)	24(3)
C(36)	2171(3)	1389(7)	4395(6)	24(3)
C(37)	2128(3)	475(8)	4538(6)	26(3)
C(38)	1917(3)	433(8)	4910(6)	27(3)
C(39)	1829(3)	1383(7)	5000(6)	27(3)
C(40)	1622(3)	1654(8)	5345(6)	26(3)
C(41)	1147(4)	2134(9)	6179(8)	48(4)
O(1)	1378(5)	1862(12)	6723(9)	48(5)

<sup>a</sup> Equivalent isotropic  $U$  defined as one-third of the trace of the orthogonalized  $U_{ij}$  tensor.

This effect was first observed by Hans Fischer<sup>36</sup> and used elegantly by Woodward in his landmark chlorophyll synthesis.<sup>37</sup> The first structural proof for steric crowding was provided during structural studies on OEP derivatives bearing a large *meso*-substituent.<sup>38</sup> Dodecasubstituted nonplanar porphyrin macrocycles are currently under active scrutiny<sup>35,39</sup> and evidence for "localized" macrocycle distortion in mono- and di-*meso*-substituted porphyrins has been described by us and others.<sup>5b,6c,40</sup>

(36) Fischer, H.; Orth, H. *Die Chemie des Pyrrols*; Akademische Verlagsgesellschaft: Leipzig, Germany, 1937; 1. Aufl.; Bd. II/1, p 144.

(37) Woodward, R. B. *Angew. Chem.* **1960**, *72*, 651; *Ind. Chim. Belge* **1962**, 1293.

(38) Hursthouse, M. B.; Neidle, S. *J. Chem. Soc., Chem. Commun.* **1972**, 449. Fuhrhop, J.-H.; Witte, L.; Sheldrick, W. S. *Liebigs Ann. Chem.* **1976**, 1537.

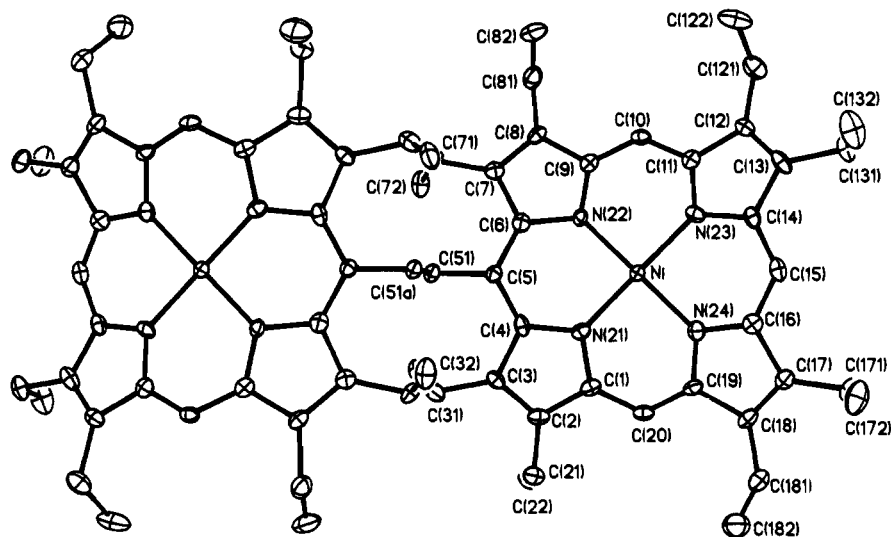


**Figure 8.** Computer generated plot and numbering scheme of the nickel *trans*-dimer, **7**. Ellipsoids are drawn for 50% occupancy; hydrogen atoms have been omitted for clarity.

**Structure of 1,2-Bis[5-(2,3,7,8,12,13,17,18-octaethylporphyrinato)nickel(II)]-*cis*-ethene, **5**.** The molecular structure of **5** is shown in Figure 5. Atomic coordinates are listed in Table 3, while selected bond lengths and angles are compiled in Table 6. Overall the structure is rather similar to the corresponding copper(II) derivative (**4**). However significant differences in the macrocycle conformation and especially the geometry of the  $\pi$ -interactions are observed.

Even a rudimentary inspection of the overlap of the  $\pi$ -systems shows a lesser degree of overlap in **5** when compared with the Cu(II) derivative (**4**) (Figure 6). The respective structural data for the intramolecular aggregate are as follows: Ni–Ni separation, 5.112 Å; center-to-center distance, 5.145 Å; slip angle, 47.1°; 4N-plane separation, 3.502 Å. This leads to a lateral shift of the centers of 3.769 Å which is 0.537 Å larger than the one observed in the copper dimer (**4**). Together with an interplanar spacing which is 0.144 Å larger than in the Cu(II) structure this clearly shows the more widened structure of the nickel(II) dimer. Thus the aggregation strength is smaller in the Ni(II) derivative than in the Cu(II) derivative. This is in line with the results on the solution aggregation of monomeric, asymmetric metalloporphyrins.<sup>25</sup>

The average Ni–N bond length in **5** is 1.925(3) Å which agrees well with the data from the tetragonal (ruffled) Ni<sup>II</sup>OEP modification [1.929(3) Å]<sup>41a</sup> but is longer than those bonds observed in the two triclinic (planar) Ni<sup>II</sup>OEP phases.<sup>41b,42</sup> A closer inspection of the individual Ni–N bond lengths shows however that significant difference between bonds occur, the longest being 1.937(4) Å for Ni(2)–N(27) and the shortest bond being Ni(2)–N(26) with 1.903(3) Å. Such differences might

be interpreted as the results of the aggregation and packing forces as has been suggested by Scheidt and co-workers.<sup>32b,42</sup> The bond lengths and bond angles of most of the macrocycle atoms and peripheral substituents agree well with data for other related metalloporphyrins.<sup>22</sup>

The pyrrole rings in macrocycle 1 are tilted on average by 16.7° against the 4N-plane; in macrocycle 2 this average angle is 17.8°. Although slight differences in the displacement of individual atoms are observed the overall conformation is similar in both macrocycles of the nickel dimer (Figure 7). The average deviation from planarity for the 24 macrocycle atoms is 0.264 Å for ring 1 and 0.279 for ring 2, respectively. The conformation is similar that found in the ruffled form of Ni<sup>II</sup>OEP<sup>41a</sup> with an alternating displacement of the *meso*-carbons by 0.54 Å (ring 1) and 0.547 Å (ring 2) above and below the mean plane. Again statistically significant differences in the displacement of the substituted and unsubstituted *meso*-positions are observed (Figure 7C,D), although they are not as drastic as observed in the copper dimer.

**Structure of 1,2-Bis[5-(2,3,7,8,12,13,17,18-octaethylporphyrinato)nickel(II)]-*trans*-ethene, **7**.** The molecular structure is shown in Figure 8, while atomic coordinates are listed in Table 4. The molecule is situated on a crystallographic inversion point; thus the asymmetric unit contains only half of the dimer and a molecule of solvation (toluene). Thus the molecule has an extended linear structure and the two porphyrin units of the bis-porphyrin are clearly connected by a *trans*-double bond with a –CH=CH distance of 1.311(10) Å. Selected bond lengths and angles are compiled in Table 6. In general there is good agreement between the structural data of the nickel(II) macrocycles in the *cis*- (**5**) and *trans*-structure (**7**) (see Table 6). The average Ni–N bond length is 1.914(5) Å which is slightly shorter than that observed in the *cis*-structure; variations in the individual bond lengths are again observed. Again the overall structural characteristics of the macrocycle atoms agree well with those of related monomeric porphyrins.<sup>22,41</sup> Notable differences are the smaller angles at the connecting *meso*-carbon atoms [C(4)–C(5)–C(6) angle] which are also observed in the corresponding Cu(II) and Ni(II) *cis*-structures. The average C<sub>a</sub>–C<sub>m</sub>–C<sub>a</sub> angle of all three Ni(II) macrocycles (ring 1 and 2 in **5** and **7**) is 121.2° for the *meso*-substituted C5 group while the average angle of all three unsubstituted *meso* groups (C10, C15, C20) is 123.7°. The relevant angle for (unsubstituted) *meso*-positions in Ni(II)OEP is 124°.<sup>41,42</sup> This is due to local steric “overloading” which is partially relieved

- (39) Barkigia, K. M.; Berber, M. D.; Fajer, J.; Medforth, C. J.; Renner, M. R.; Smith, K. M. *J. Am. Chem. Soc.* **1990**, *112*, 8851. Medforth, C. J.; Senge, M. O.; Smith, K. M.; Sparks, L. D.; Shelnut, J. A. *J. Am. Chem. Soc.* **1992**, *114*, 9859. Mandon, D.; Ochsenbein, P.; Fischer, J.; Weiss, R.; Jayaraj, K.; Austin, R. N.; Gold, A.; White, P. S.; Brigaud, O.; Battioni, P.; Mansuy, D. *Inorg. Chem.* **1992**, *31*, 2044. Senge, M. O.; Medforth, C. J.; Sparks, L. D.; Shelnut, J. A.; Smith, K. M. *Inorg. Chem.* **1993**, *32*, 1716. Bhyrappa, P.; Krishnan, V.; Nethaji, M. *J. Chem. Soc., Dalton Trans.* **1993**, 1901. Senge, M. O. *J. Chem. Soc., Dalton Trans.* **1993**, 3539.
- (40) Senge, M. O.; Vicente, M. G. H.; Parkin, S. R.; Hope, H.; Smith, K. M. *Z. Naturforsch.* **1992**, *47b*, 1189. Senge, M. O. *J. Photochem. Photobiol. B: Biol.* **1992**, *16*, 3. Senge, M. O.; Smith, N. W.; Smith, K. M. *Inorg. Chem.* **1993**, *32*, 1259.
- (41) (a) Meyer, E. F., Jr. *Acta Crystallogr., Sect. B* **1972**, *28*, 2162. (b) Cullen, D. L.; Meyer, E. F., Jr. *J. Am. Chem. Soc.* **1974**, *96*, 2095.
- (42) Brennan, T. D.; Scheidt, W. R.; Shelnut, J. A. *J. Am. Chem. Soc.* **1988**, *110*, 3919.

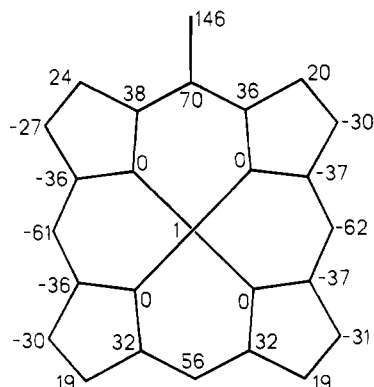


**Figure 9.** Deviations from the least-squares 4N-plane for the nickel dimer, 7 [ $\text{\AA} \times 10^2$ ].

by smaller bond angles and out-of-plane distortion. This effect has already been noted in conjunction with ongoing studies on nonplanar porphyrins.<sup>39,40</sup>

The structure exhibits the typical  $S_4$ -ruffled core found in many Ni(II) (Figure 9).<sup>5b,22,41,42</sup> The average deviation of the 24 macrocycle atoms from planarity is 0.307  $\text{\AA}$  with the *meso*-carbons being displaced alternately by 0.62  $\text{\AA}$  above and below their mean plane. The individual pyrrole planes are twisted on average by 19.6° against the 4N-plane. As was the case for the *cis*-dimer (5) a slightly larger displacement is observed for the substituted *meso*-carbon, C(5). In general the structure is rather similar to the one of 1,2-bis[5-(2,3,7,8,12,13,17,18-octaethylporphyrinato)nickel(II)]ethane described by Hitchcock which contains an ethane bridge.<sup>5b</sup> Recently Kitagawa et al. described the crystal structure of the chloroform solvate of 7.<sup>19b</sup> The overall structural characteristics are similar to the one described here for the toluene solvate.

**Structure of Nickel Carbinol Dimer, 13.** The molecular structure of 13 is shown in Figure 10, while atomic coordinates and isotropic thermal parameters are listed in Table 5. The structure reveals clearly that low-valent titanium coupling of some  $\beta$ -formyl-substituted porphyrins proceeds not via formation of a connecting double bond, as was observed for *meso*-formyl porphyrins, but rather leads to the formation of carbinol-bridged bisporphyrins. In contrast to the structures of the *cis*- or *trans*-ethylene-bridged dimers, which have more or less

coplanar macrocycle arrangements, here the two macrocycles form a skewed structure. The two macrocycles are considerably rotated against each other; the angle between the two nitrogen planes is 77.3°. The distance between the two nickel centers is 8.076  $\text{\AA}$ . The structure is only of marginal quality with high *esd*'s for the bond angles and lengths and unsatisfactorily high *R*-values. Therefore Table 7 lists only the data on the metal coordination. The Ni–N bond lengths are on average 1.953(5)  $\text{\AA}$  and thus compare well with the triclinic Ni<sup>II</sup>OEP modifications.<sup>41b,42</sup> These bond lengths are significantly larger than those observed for the *cis*- or *trans*-ethene bridged dimers 5 and 7 which can be explained by the lesser degree of ruffling in 13. While the average deviation from planarity is 0.18  $\text{\AA}$  for the 24 macrocycle atoms in macrocycle 1, macrocycle 2 is much less distorted with an average deviation from its least-squares plane of 0.06  $\text{\AA}$ . The different degree of distortion is also evidenced by the average displacement of the *meso*-carbons from the 4N-plane. For macrocycle 1 the *meso*-carbons are alternately displaced by 0.35  $\text{\AA}$  above and below the 4N-plane while the respective value for macrocycle 2 is 0.1  $\text{\AA}$ . No significant differences in the degree of displacement are observed between individual *meso*-carbons. A more detailed inspection of the structural parameters is impeded by the poor resolution.

**Intermolecular Aggregation and Crystal Packing.** Besides the strong intramolecular packing described above for the *cis*-ethene-bridged bisporphyrins all structures described here exhibited intermolecular aggregation between the macrocycles. Both the copper (4) (not shown) and nickel (5) *cis*-ethene dimers have similar packing patterns. The packing is characterized by the formation of well separated stacks of molecules. In these stacks dimeric structures of the bisporphyrins are observed, i.e. the dimers interact by  $\pi$ -aggregation effects. Medium strength  $\pi$ -aggregation is observed between neighboring macrocycles of (different dimers) within these stacks. The macrocycle involved in these dimers is the one containing Cu(2). The Cu–Cu separation is 4.906  $\text{\AA}$  and the center-to-center separation is 4.914  $\text{\AA}$ . The mean plane separation of the neighboring macrocycles is 3.48  $\text{\AA}$ ; this is slightly less than in the intramolecular aggregate structure. The slip angle is 44.9°, which leads to a lateral shift of the center of 3.469  $\text{\AA}$ . Thus with a slightly smaller plane separation and a slightly larger lateral shift the aggregate strength

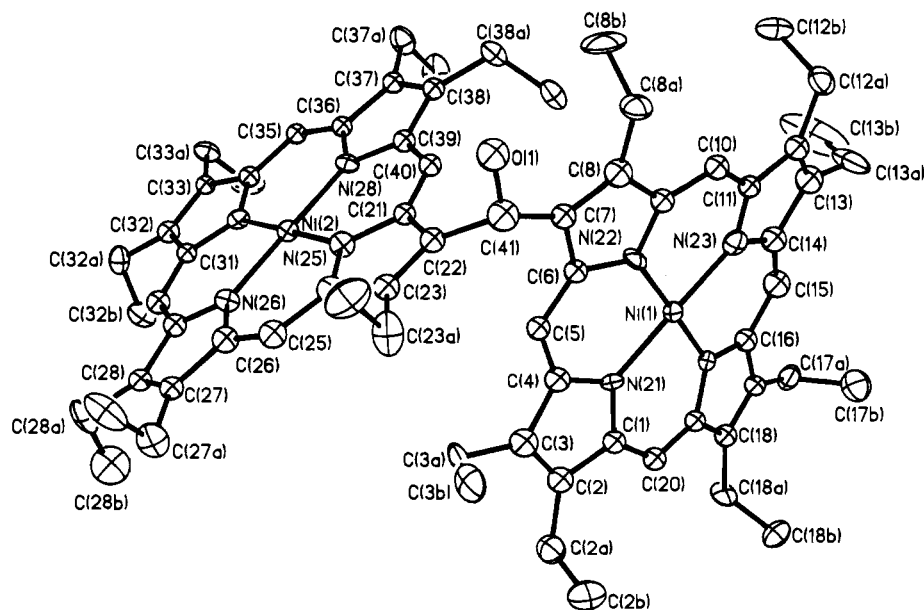


**Figure 10.** Computer-generated plot and numbering scheme of the nickel carbinol dimer 13. Ellipsoids are drawn for 40% occupancy; hydrogen atoms, the disordered positions, and the second position of the carbinol-oxygen atom have been omitted for clarity.

**Table 6.** Selected Bond Lengths (Å) and Angles (deg) for Compounds 4, 5, and 7

	4, M = Cu(II)		5, M = Ni(II)		7, M = Ni(II)
	macrocycle 1	macrocycle 2	macrocycle 1	macrocycle 2	
M(1)–N(21)	1.995(3)	1.997(3)	1.918(3)	1.929(4)	1.913(5)
M(1)–N(22)	1.997(2)	1.999(2)	1.931(3)	1.903(3)	1.901(4)
M(1)–N(23)	1.996(3)	1.998(3)	1.927(3)	1.937(4)	1.922(5)
M(1)–N(24)	1.997(2)	1.999(2)	1.935(3)	1.917(3)	1.921(4)
N(21)–C(1)	1.376(4)	1.375(5)	1.382(5)	1.377(6)	1.380(6)
N(21)–C(4)	1.374(4)	1.376(4)	1.376(5)	1.386(5)	1.395(6)
N(22)–C(6)	1.375(5)	1.377(4)	1.391(6)	1.379(5)	1.394(6)
N(22)–C(9)	1.375(4)	1.377(5)	1.370(5)	1.385(5)	1.385(8)
N(23)–C(11)	1.375(4)	1.376(5)	1.364(5)	1.381(5)	1.376(7)
N(23)–C(14)	1.375(3)	1.377(4)	1.385(6)	1.387(5)	1.391(5)
N(24)–C(16)	1.375(4)	1.377(4)	1.372(5)	1.388(6)	1.374(6)
N(24)–C(19)	1.377(4)	1.376(5)	1.373(5)	1.366(6)	1.375(7)
C(1)–C(2)	1.443(6)	1.438(6)	1.436(6)	1.441(6)	1.430(8)
C(1)–C(20)	1.388(5)	1.381(5)	1.376(6)	1.368(6)	1.380(6)
C(2)–C(3)	1.370(5)	1.373(5)	1.354(6)	1.363(6)	1.366(6)
C(3)–C(4)	1.459(6)	1.457(6)	1.447(5)	1.471(7)	1.460(8)
C(4)–C(5)	1.407(5)	1.406(6)	1.403(5)	1.390(6)	1.379(6)
C(5)–C(6)	1.408(6)	1.400(6)	1.395(6)	1.394(6)	1.392(8)
C(6)–C(7)	1.463(5)	1.463(5)	1.459(6)	1.458(5)	1.456(7)
C(7)–C(8)	1.358(6)	1.355(6)	1.357(7)	1.360(6)	1.371(8)
C(8)–C(9)	1.441(5)	1.445(5)	1.431(6)	1.440(6)	1.436(6)
C(9)–C(10)	1.380(6)	1.378(5)	1.377(6)	1.380(6)	1.372(7)
C(10)–C(11)	1.375(5)	1.382(5)	1.376(6)	1.373(6)	1.382(6)
C(11)–C(12)	1.446(6)	1.437(5)	1.440(6)	1.448(6)	1.442(7)
C(12)–C(13)	1.349(5)	1.350(5)	1.357(7)	1.358(6)	1.357(7)
C(14)–C(15)	1.401(5)	1.406(6)	1.369(6)	1.364(6)	1.370(7)
C(13)–C(14)	1.448(5)	1.449(6)	1.450(6)	1.425(6)	1.429(8)
C(15)–C(16)	1.387(5)	1.386(7)	1.377(6)	1.355(7)	1.376(8)
C(16)–C(17)	1.440(5)	1.441(6)	1.448(6)	1.443(6)	1.451(7)
C(17)–C(18)	1.341(6)	1.373(6)	1.360(6)	1.344(8)	1.364(7)
C(18)–C(19)	1.455(5)	1.450(5)	1.446(6)	1.442(6)	1.454(6)
C(19)–C(20)	1.366(6)	1.375(6)	1.376(6)	1.375(7)	1.371(7)
C(5)–CH=	1.489(7)	1.489(6)	1.479(7)	1.479(6)	1.502(7)
–CH=CH–		1.327(7)		1.339(7)	1.311(10)
N(21)–M(1)–N(22)	88.9(1)	89.2(1)	88.4(1)	89.2(1)	89.4(2)
N(21)–M(1)–N(23)	179.3(1)	173.8(1)	179.3(2)	177.0(2)	179.2(2)
N(22)–M(1)–N(23)	90.8(1)	91.0(1)	91.5(1)	90.7(1)	90.7(2)
N(21)–M(1)–N(24)	90.6(1)	90.8(1)	91.2(1)	90.5(1)	90.4(2)
N(22)–M(1)–N(24)	179.5(1)	179.8(1)	178.5(2)	179.5(2)	179.3(2)
N(23)–M(1)–N(24)	89.7(1)	89.0(1)	88.9(1)	89.6(1)	89.5(2)
M(1)–N(21)–C(1)	126.2(2)	125.8(2)	125.8(3)	125.8(3)	127.1(3)
M(1)–N(21)–C(4)	127.4(2)	128.7(2)	129.3(2)	128.3(3)	127.4(3)
C(1)–N(21)–C(4)	106.3(3)	105.6(3)	104.8(3)	105.8(4)	105.5(4)
M(1)–N(22)–C(6)	128.0(2)	128.0(2)	129.0(3)	128.1(3)	128.6(4)
M(1)–N(22)–C(9)	125.6(2)	126.2(2)	125.7(3)	126.6(3)	126.6(3)
C(6)–N(22)–C(9)	106.1(3)	105.8(3)	105.2(3)	105.2(3)	104.8(4)
M(1)–N(23)–C(11)	126.7(2)	126.6(2)	126.8(3)	127.3(3)	127.0(3)
M(1)–N(23)–C(14)	127.6(2)	128.0(3)	128.5(3)	127.6(3)	128.2(4)
C(11)–N(23)–C(14)	105.7(3)	105.0(3)	104.8(3)	104.7(3)	104.7(4)
M(1)–N(24)–C(16)	127.5(2)	128.5(3)	128.3(3)	127.2(3)	127.5(3)
M(1)–N(24)–C(19)	126.7(2)	127.1(2)	126.7(3)	127.8(3)	126.7(3)
C(16)–N(24)–C(19)	105.7(3)	104.4(3)	105.0(3)	105.1(3)	105.7(4)
N(21)–C(1)–C(2)	110.4(3)	110.6(3)	110.7(4)	110.7(4)	111.1(4)
N(21)–C(1)–C(20)	124.6(4)	125.9(4)	124.8(4)	125.2(4)	123.9(5)
C(2)–C(1)–C(20)	124.8(3)	123.6(4)	124.3(4)	123.6(4)	124.6(5)
C(1)–C(2)–C(3)	106.7(3)	104.4(4)	107.1(3)	107.5(4)	107.1(4)
C(2)–C(3)–C(4)	106.6(3)	105.4(3)	106.3(4)	106.1(4)	106.8(4)
N(21)–C(4)–C(3)	109.8(3)	110.8(3)	110.9(3)	109.8(4)	109.4(4)
N(21)–C(4)–C(5)	124.3(4)	123.5(4)	123.7(3)	123.5(4)	123.9(5)
C(3)–C(4)–C(5)	125.9(3)	125.5(3)	125.4(4)	126.6(4)	126.4(4)
C(4)–C(5)–C(6)	123.3(4)	123.6(4)	121.2(4)	120.4(4)	122.1(4)
N(22)–C(6)–C(5)	123.3(3)	124.6(3)	122.8(4)	124.8(3)	122.8(4)
N(22)–C(6)–C(7)	110.0(3)	109.8(3)	109.8(4)	110.5(4)	110.5(5)
C(5)–C(6)–C(7)	126.6(3)	125.6(3)	127.3(4)	124.4(4)	126.4(4)
C(6)–C(7)–C(8)	106.1(3)	106.9(3)	106.4(4)	106.3(4)	106.3(4)
C(7)–C(8)–C(9)	107.5(3)	106.7(3)	107.2(4)	107.2(4)	107.1(5)
N(22)–C(9)–C(8)	110.2(3)	110.8(3)	125.3(4)	110.7(4)	111.3(5)
N(22)–C(9)–C(10)	125.3(3)	124.9(3)	125.3(4)	125.0(4)	124.5(4)
C(8)–C(9)–C(10)	123.8(3)	124.3(4)	122.8(4)	124.2(4)	123.9(5)
C(9)–C(10)–C(11)	126.4(4)	126.7(4)	123.8(4)	124.2(4)	123.7(5)
N(23)–C(11)–C(10)	124.3(4)	124.1(3)	124.5(4)	123.1(4)	123.5(5)
N(23)–C(11)–C(12)	109.9(3)	110.9(3)	111.6(4)	111.2(3)	111.0(4)

Table 6 (Continued)

	4, M = Cu(II)		5, M = Ni(II)		7, M = Ni(II)
	macrocycle 1	macrocycle 2	macrocycle 1	macrocycle 2	
C(10)–C(11)–C(12)	125.7(3)	125.0(4)	123.7(4)	125.5(4)	125.1(5)
C(11)–C(12)–C(13)	107.5(3)	107.0(4)	106.6(4)	105.4(4)	106.3(5)
C(12)–C(13)–C(14)	106.4(3)	106.6(3)	106.4(4)	108.4(4)	107.4(4)
N(23)–C(14)–C(13)	110.5(2)	110.6(3)	110.6(4)	110.3(3)	110.4(4)
N(23)–C(14)–C(15)	124.4(1)	124.5(4)	124.2(4)	123.7(4)	123.0(5)
C(13)–C(14)–C(15)	125.1(2)	125.0(3)	125.0(4)	125.8(4)	126.1(4)
C(14)–C(15)–C(16)	125.7(2)	125.7(4)	123.0(4)	124.0(4)	123.7(4)
N(24)–C(16)–C(15)	124.3(3)	123.8(3)	124.6(4)	124.2(4)	124.4(4)
N(24)–C(16)–C(17)	110.3(3)	112.0(4)	110.9(3)	109.9(4)	110.5(4)
C(15)–C(16)–C(17)	125.3(3)	123.9(3)	124.1(4)	124.5(4)	124.6(4)
C(16)–C(17)–C(18)	107.2(3)	105.9(3)	106.6(4)	107.1(4)	106.8(4)
C(17)–C(18)–C(19)	107.0(3)	106.3(4)	106.2(3)	106.7(4)	106.2(4)
N(24)–C(19)–C(18)	109.7(3)	111.4(3)	111.2(3)	111.0(4)	110.7(4)
N(24)–C(19)–C(20)	124.4(3)	124.2(3)	124.1(4)	124.0(4)	124.4(4)
C(18)–C(19)–C(20)	125.9(3)	124.3(4)	124.6(4)	124.7(4)	124.6(5)
C(1)–C(20)–C(19)	126.6(4)	126.2(4)	124.2(4)	123.5(4)	123.6(4)
C(4)–C(5)–CH=	118.1(4)	116.2(4)	120.2(4)	118.3(4)	119.5(5)
C(6)–C(5)–CH=	118.0(3)	119.2(4)	118.5(4)	121.1(4)	118.4(4)
C(5)–CH=CH–	121.9(4)	123.8(4)	123.3(4)	124.1(4)	121.7(5)

Table 7. Selected Bond Lengths (Å) and Angles (deg) for the Nickel Carbinol Dimer, 13

Ni(1)–N(21)	1.952(4)	Ni(1)–N(22)	1.953(5)
Ni(1)–N(23)	1.953(4)	Ni(1)–N(24)	1.952(5)
Ni(2)–N(25)	1.953(6)	Ni(2)–N(26)	1.953(4)
Ni(2)–N(27)	1.952(6)	Ni(2)–N(28)	1.953(3)
C(7)–C(41)	1.54(2)	C(22)–C(41)	1.55(2)
C(41)–O(1)	1.321(2)		
N(21)–Ni(1)–N(22)	90.6(3)	N(21)–Ni(1)–N(23)	179.3(4)
N(22)–Ni(1)–N(23)	89.8(3)	N(21)–Ni(1)–N(24)	89.0(3)
N(22)–Ni(1)–N(24)	178.1(3)	N(23)–Ni(1)–N(24)	90.6(3)
Ni(1)–N(21)–C(1)	127.1(6)	Ni(1)–N(21)–C(4)	125.4(6)
Ni(1)–N(22)–C(6)	127.7(6)	Ni(1)–N(22)–C(9)	127.1(6)
Ni(1)–N(23)–C(11)	127.9(6)	Ni(1)–N(23)–C(14)	127.0(7)
Ni(1)–N(24)–C(16)	127.9(6)	Ni(1)–N(24)–C(19)	128.6(6)
C(6)–C(7)–C(41)	125(1)	C(8)–C(7)–C(41)	126(1)
N(25)–Ni(2)–N(27)	179.0(3)	N(26)–Ni(2)–N(27)	89.8(4)
N(25)–Ni(2)–N(28)	90.2(4)	N(26)–Ni(2)–N(28)	179.1(4)
N(27)–Ni(2)–N(28)	89.7(4)	Ni(2)–N(25)–C(21)	127.7(7)
Ni(2)–N(25)–C(24)	127.6(8)	Ni(2)–N(26)–C(26)	129.0(8)
Ni(2)–N(26)–C(29)	127.8(8)	Ni(2)–N(27)–C(31)	128.5(7)
Ni(2)–N(27)–C(34)	127.6(7)	Ni(2)–N(28)–C(36)	128.7(8)
Ni(2)–N(28)–C(39)	126.8(8)	C(21)–C(22)–C(41)	126(1)
C(23)–C(22)–C(41)	125(1)	C(7)–C(41)–C(22)	113(1)
C(7)–C(41)–O(1)	116(1)	C(22)–C(41)–O(1)	110(1)

in the intermolecular  $\pi$ -aggregated dimer is comparable to that found in the intramolecularly aggregated *cis* bisporphyrin.

The molecular packing (Figure 11) in the nickel *cis*-ethene dimer (5) is similar to the situation found for the corresponding copper(II) derivative (4). The Ni–Ni separations between neighboring stacks are 12.24 and 12.45 Å. Evidence for intermolecular  $\pi$ -interaction is found again, although to a much lesser degree than in the case of the copper compound (4). The Ni–Ni separation between neighboring macrocycles in a given stack is 6.22 Å with a center-to-center distance of 6.18 Å. The two 4N-planes are separated by 3.94 Å. The slip angle between the related centers is 50.4°, leading to a lateral shift of the centers of 4.763 Å. Thus, as was the case for the intramolecular aggregation, less intermolecular aggregation is found for the nickel *cis*-dimer (5) in the solid state when compared with its copper(II) counterpart (4).

While in the case of the *cis*-ethene-bridged bisporphyrins intramolecular aggregation was found, no such interaction is possible for the *trans*-ethene dimer (7). However, again intermolecular aggregation typical for metalloporphyrins was found. Figure 12 shows a view of the unit cell of 7 and indicates that some overlap exists between neighboring macrocycles. The

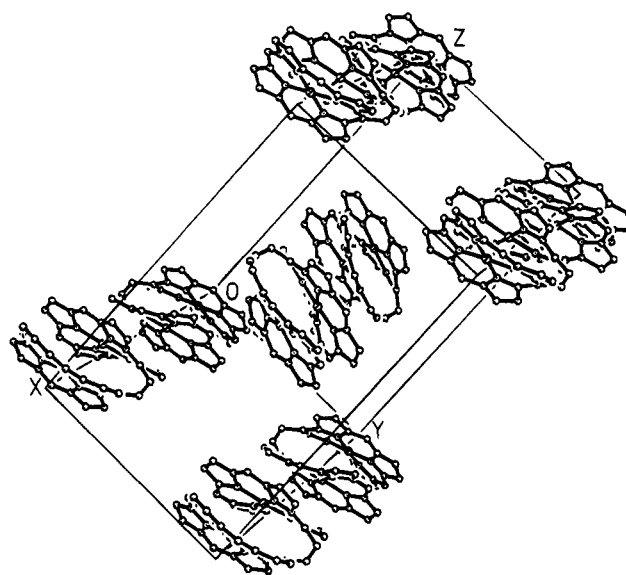
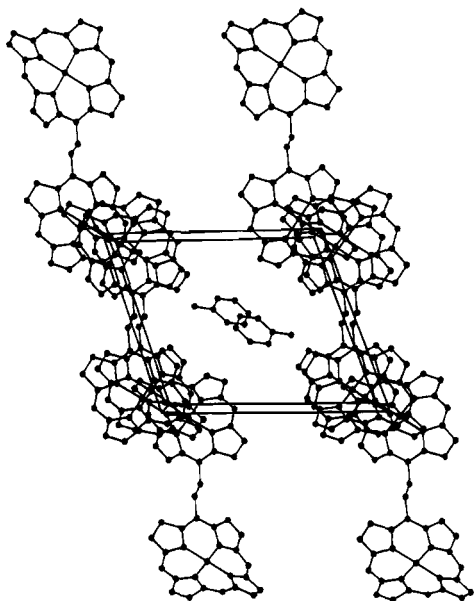


Figure 11. View of the molecular packing in the crystal of nickel *cis*-dimer, 5. Hydrogen atoms and ethyl side chains have been omitted for clarity.

packing is characterized by the formation of parallel running stacks which are well separated by the incorporation of solvent molecules (toluene) in the void between the layers. In the third dimension the layers are not exactly top-over-top but are shifted sideways in a staircase-like arrangement. Two different types of intermolecular aggregates are formed, which differ mainly in the degree of overlap of the  $\pi$ -systems and the interplanar separation. One structure exhibits intermediate<sup>22</sup> strength aggregation with a Ni–Ni separation of 5.767 Å, a center-to-center distance of 5.756 Å, a mean plane separation of 3.922 Å, and a slip angle of 47.1°. This leads to a value of 4.217 Å for the lateral shift of the centers. The second aggregate structure is of weaker strength with a Ni–Ni separation of 7.131 Å, a center-to-center distance of 7.141 Å, a slip angle of 45.9°, and an interplanar distance of 4.972 Å. The lateral shift for this arrangement is 5.128 Å. The geometrical data described here for the “stronger” aggregate are in line with data observed for a variety of intermediate-to-weak strength aggregates described in the literature.<sup>43</sup>

(43) See ref 22 for a list of all structures up to 1987. Senge, M. O.; Smith, K. M. *Z. Naturforsch.* **1993**, *48b*, 821. Senge, M. O.; Hope, H.; Iakovides, P.; Smith, K. M. *Photochem. Photobiol.* **1993**, *58*, 748.



**Figure 12.** View of the molecular packing in the crystal of nickel *trans*-dimer, **7**. Hydrogen atoms and ethyl side chains have been omitted for clarity.

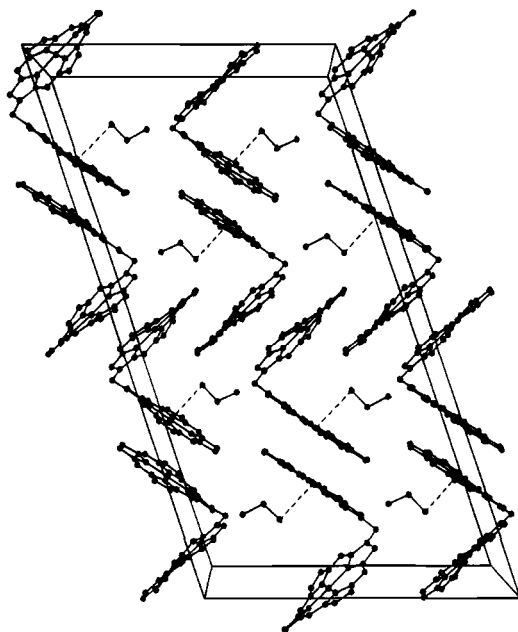


**Figure 13.** View of the molecular packing (down *b*-axis) in the crystal of nickel *carbinol* dimer, **13**. Hydrogen atoms and ethyl side chains have been omitted for clarity. Dashed lines indicated the contacts between the dichloromethane solvate molecule and nickel centers.

Figure 13 shows a view of the molecular packing of the nickel *carbinol* dimer **13**. The dimers pack very closely on one side with considerable overlap of the  $\pi$ -systems. Thus, dimeric aggregates of bisporphyrins are formed. The formation of extended  $\pi$ -stacked aggregates is prevented by solvent molecules (methylene chloride) which are situated other (nonaggregated) side of the macrocycle. The distance between the chlorine atom of the solvate molecule and Ni(2) is 3.67 Å; this arrangement effectively blocks the second face of the macrocycle for aggregation. Figure 14 shows the degree of overlap between two neighboring macrocycles with Ni(2). The Ni–Ni distance is 4.688 Å while the center-to-center distance is 4.703 Å. Close interaction is already indicated by the small interplanar separa-

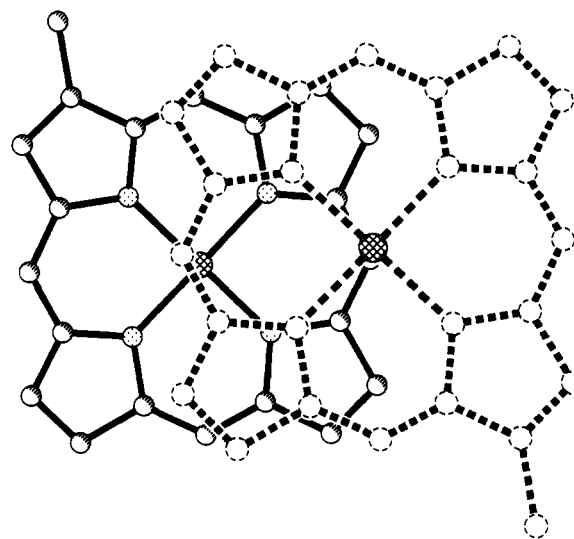


**Figure 14.** Top view of the intermolecular  $\pi$ -dimers formed in the crystal of the nickel *carbinol* dimer, **13**. Only the macrocycle atoms and the connecting *carbinol* carbons are shown. The 4N-plane of the upper macrocycle (dashed) is in the plane of the paper.

tion of 3.396 Å. The slip angle between the two centers is 43.8° which leads to a lateral shift of the centers of 3.255 Å. Note that these values are only marginally larger than those observed for the strong intramolecular  $\pi$ -stacked copper *cis*-ethene dimer **4**.

## Conclusions

The synthesis of face-to-face bisporphyrins is readily achieved in a single step reaction with reasonable yields from the corresponding formylporphyrins. This provides a considerable improvement over more laborious total synthesis approaches to bisporphyrins and allows the preparation of cofacial porphyrins on a large scale. The bisporphyrins prepared by the McMurry reaction have coplanar macrocycle arrangements with considerable overlap of the  $\pi$ -systems and show intramolecular aggregation. In addition, studies of the molecular packing revealed the formation of intermolecular aggregates. Differences in the spatial structure of the copper and nickel *cis*-ethene dimers indicate the possibility to modulate the interplanar distance and aggregation strength with different metal ions. Variation of the relative macrocycle arrangement can either be achieved by isomerization of the *cis*-ethene bridged dimers to the *trans* compounds to yield bisporphyrins with extended structures. The *trans* compound can also be obtained as an easily separated side product of the coupling reaction. Coupling of a  $\beta$ -formylporphyrin yields gable-type *carbinol*-bridged bisporphyrins. Thus by simple variation of the basic starting material and/or the reaction conditions three bisporphyrin types with either cofacial, linear or gable-type macrocycle arrangement can be prepared.

**Acknowledgment.** This work was supported by grants from the Deutsche Forschungsgemeinschaft to M.O.S. and the National Institutes of Health to K.M.S. (HL-22252).

**Supplementary Material Available:** Listings of data collection parameters and complete bond lengths, bond angles, anisotropic thermal parameters, and hydrogen atom coordinates and *B* values for compounds **5** and **7** (16 pages). Ordering information is given on any current masthead page. For supplementary material of compounds **4** and **13**, see ref 12.